



The Pignola-Abriola section (southern Apennines, Italy): a new GSSP candidate for the base of the Rhaetian Stage

MANUEL RIGO, ANGELA BERTINELLI, GIUSEPPE CONCHERI, GIOVANNI GATTOLIN, LINDA GODFREY, MIRIAM E. KATZ, MATTEO MARON, PAOLO MIETTO, GIOVANNI MUTTONI, MARIO SPROVIERI, FABIO STELLIN AND MARIACHIARA ZAFFANI

LETHAIA



Rigo, M., Bertinelli, A., Concheri, G., Gattolin, G., Godfrey, L., Katz, M.E., Maron, M., Mietto, P., Muttoni, G., Sprovieri, M., Stellin, F. & Zaffani, M. 2016: The Pignola-Abriola section (southern Apennines, Italy): a new GSSP candidate for the base of the Rhaetian Stage. *Lethaia*, Vol. 49, pp. 287–306.

The base of the Rhaetian stage (Norian/Rhaetian boundary, NRB) is still awaiting formal designation by the International Commission on Stratigraphy. At present, only the 4.30-m-thick Steinbergkogel section (Austria) has been proposed as GSSP (Global Stratotype Section and Point) candidate for the base of the Rhaetian. Here we present data from the 63-m-thick Pignola-Abriola section (Southern Apennines, Italy) that we consider an alternative candidate for the Rhaetian GSSP. The Pignola-Abriola basal section, represented by hemipelagic–pelagic carbonate successions belonging to the Lagonegro Basin, matches all the requirements for a GSSP: 1, it is well exposed with minimal structural deformation; 2, it is rich in age diagnostic fossils (e.g. conodonts and radiolarians); 3, it yields a geochemical record suitable for correlation (e.g. $\delta^{13}\text{C}_{\text{org/carb}}$); and 4, it has a robust magnetostratigraphy and is correlated with the Newark APTS for age approximation of the NRB and additional Rhaetian bioevents. In the Pignola-Abriola section, we opt to place the NRB at the 44.4 metre level, coincident with a prominent negative shift of ca. 6‰ of the $\delta^{13}\text{C}_{\text{org}}$. This level is located 50 cm below the FAD of conodont *Misikella posthernsteini* s.s within the radiolarian *Proparvicungula moniliformis* Zone. Both the negative $\delta^{13}\text{C}_{\text{org}}$ shift and the FAD of *Misikella posthernsteini* occur within Pignola-Abriola magnetozone MPA-5r, at ~205.7 Ma, according to magnetostratigraphical correlation to the Newark APTS. We also illustrate the coeval Mt. Volturino stratigraphical section deposited below the calcite compensation depth (CCD) within the same Lagonegro Basin and characterized by a detailed radiolarian biostratigraphy and strong $\delta^{13}\text{C}_{\text{org}}$ negative shift around the NRB. □ Conodonts, GSSP, Late Triassic, magnetostratigraphy, radiolarians, Rhaetian, stable isotopes.

Manuel Rigo [manuel.rigo@unipd.it], Giovanni Gattolin [gio.gattolin@gmail.com], Matteo Maron [matteo.maron.1@studenti.unipd.it], Paolo Mietto [paolo.mietto@unipd.it], Mariachiara Zaffani [mariachiara.zaffani@studenti.unipd.it], Department of Geosciences, University of Padova, via Gradenigo 6, 35131 Padova, Italy; Angela Bertinelli [angela.bertinelli@unipg.it], Department of Physics and Geology, University of Perugia, via Pascoli, 06123 Perugia, Italy; Giuseppe Concheri [giuseppe.concheri@unipd.it], Fabio Stellin [fabio.stellin@studenti.unipd.it], Department of Agronomy Food Natural Resources Animals and Environment, University of Padova, Viale dell'Università 16, 35020 Legnaro, Padova, Italy; Giovanni Gattolin [gio.gattolin@gmail.com], ENI E&P division, via Emilia 1 20097, San Donato Milanese, Italy; Linda Godfrey [godfrey@marine.rutgers.edu], Department Earth and Planetary Sciences, Rutgers University, Piscataway, NJ 08854, USA; Miriam E. Katz [katzm@rpi.edu], Department of Earth and Environmental Sciences, Rensselaer Polytechnic Institute, 110 8th St., Troy, NY 12180, USA; Giovanni Muttoni [giovanni.muttoni1@unimi.it], Department of Earth Sciences 'Ardito Desio', University of Milano, via Mangiagalli 34, 20133 Milan, Italy; Mario Sprovieri [mario.sprovieri@iamc.cnr.it], IAMC-CNR, Via del Mare 3, 91021 Torretta Granitola, Trapani, Italy; Manuel Rigo [manuel.rigo@unipd.it], IGG-CNR, Via G Gradenigo 6, 35131 Padova Italy; manuscript received on 28/11/2014; manuscript accepted on 8/04/2015.

The Rhaetian was first proposed as a stage in 1891 by Carl Wilhelm Ritter von Gümbel, named after the *Raetia* Province of the Roman Empire and applied to all those strata containing the bivalve *Avicula contorta*, which was a peculiar bivalve of the shallow-marine facies of the western Tethys (such as the Kössen Beds of Austria). The Rhaetian was included as Stufe (=Stage) in the first chronostratigraphical

scale of the Triassic System by Von Mojsisovics *et al.* (1895), as 'Zone der *Avicula contorta*', and accepted as the last Stage of the Triassic by von Arthaber (1905). Since then, the Rhaetian has been subject to intense debates focusing on whether it should be recognized as an independent Stage (e.g. Pearson 1970; Ager 1987) or assigned to the Jurassic System, as suggested by Slavín (1961, 1963) for ammonoid-bar-

ren strata of northwestern Europe (a suggestion that was not met with acceptance), or included in the Norian Stage, as recommended by Tozer (1967) and Silberling & Tozer (1968) and adopted for instance by Zapfe (1974) and Palmer (1983), or even completely eradicated from geological time-scales (e.g. Tozer 1984, 1990). However, most specialists, especially those working in the Tethyan Realm, accepted the Rhaetian as a Stage of the Upper Triassic Series (e.g. Kozur & Mock 1974; Gaździcki 1978; Gaździcki et al. 1979; Krystyn 1980, 1990; Fähræus & Ryley 1989). Notably, in the *Carta Geologica Italiana* published in the 1970s and 1980s, the Rhaetian was always considered as a Stage of the Upper Triassic. In the final report of the IGCP 4 (Zapfe 1983), the Rhaetian Stage was included in the Tethyan time-scale, but not in the Canadian or Soviet Union time-scales. In 1991, the Subcommittee on Triassic Stratigraphy (STS) confirmed the Rhaetian as an independent Stage, yet a formal marker to define its base is still lacking.

Possible markers, mostly in the form of bioevents, to assign the base of the Rhaetian have been listed by Krystyn (2010) in an activity report of the Norian/Rhaetian Working Group and also reported by Ogg in Gradstein et al. (2012); these are

- FAD (First Appearance Datum) of conodont *Misikella posthernsteini*;
- Base of the *Propavicingula moniliformis* radiolarian Zone;
- FAD of conodont *Mockina mosheri* morphotype A;
- LO (Last Occurrence) of ammonoid genus *Metasibirites*;
- FAD of the ammonoid *Paracochloceras suessi*;
- Disappearance of the standard-size bivalve genus *Monotis*; and
- Prominent change from an extended normal-polarity magnetozone upward into a reversed polarity magnetozone (UT23n to UT23r), from the composite scale illustrated by Hounslow & Muttoni (2010).

At present, the only suggested GSSP candidate for the Rhaetian is represented by the Steinbergkogel section in Salzkammergut (Austria) (Krystyn et al. 2007a,b). The Steinbergkogel section, exposed in an abandoned quarry surrounded by a forested area, is comprised of red and grey, marine pelagic, condensed Hallstatt Limestone beds with ammonoids, bivalves, conodonts and other micro-fossils such as calcareous coccoliths, dinoflagellate cysts and sporomorphs (e.g. Gardin et al. 2012). This section is composed of three sub-sections named STK-A, STK-B and STK-C, with

STK-A correlative to STK-C and STK-B stratigraphically coeval. In this composite section, three events have been suggested as possible markers for the base of the Rhaetian: (1) first occurrence (FO) of *Misikella hernsteini*, corresponding to the FO of the ammonoid *Tragorhacoceras*, as well as the appearance of the genus *Rhaetites* (Krystyn et al. 2007a); (2) FAD of *Misikella posthernsteini* (Krystyn 2008), correlated to the base of the radiolarian *Propavicingula moniliformis* Zone (e.g. Kozur 2003; Giordano et al. 2010) and the FO of *Paracochloceras suessi* (Krystyn et al. 2007a); and (3) FO of the ammonoid *Cycloceltites* and *Choristoceras* and disappearance of *Sagenites*, *Dionites* and *Pinacoceras* (Krystyn et al. 2007a). Ammonoid biostratigraphy is considered one of the main tools for high-resolution dating and correlation of Triassic sedimentary sequences (Balini et al. 2010). Unfortunately, for the upper Norian and Rhaetian, ammonoids are documented only locally. For instance, the only sedimentary formation in Italy with documented (but poorly preserved) ammonoids attributed to *Choristoceras* cf. *rhaeticum* (Gümbel) is the Calcare di Chiampomano outcropping in the Preone Valley near Udine (northeastern Southern Alps) (Guembel 1861).

Conodonts and radiolarians are instead more frequent and are thus used as primary biostratigraphic tools for the definition of upper Norian and Rhaetian strata and correlations (e.g. Carter & Orchard 2007; Rigo et al. 2007, 2012a; Giordano et al. 2010).

Here, we present data from the 63-m-thick Pignola-Abriola section (Lagonegro Basin, Southern Apennines, Italy). We show that this section presents all the desirable attributes of a new, valid GSSP candidate for the base of the Rhaetian Stage. We also illustrate data from the ancillary and coeval Mt. Volturino stratigraphical section deposited in the same basin but presumably below the CCD.

Geological setting

The Pignola-Abriola and Mt. Volturino sections belong to the Lagonegro Basin succession (Southern Apennines) and are made up of hemipelagic to pelagic marine deposits. The Lagonegro Basin is considered part of the southwestern branch of the Tethys Ocean and is bordered to the north by the Apenninic and Apulian carbonate platforms (e.g. Şengör et al. 1984; Stampfli et al. 1991; Stampfli & Marchant 1995; Catalano et al. 2001; Ciarapica & Passeri 2002, 2005). The deepening-upward Lagonegro Basin suc-

cession is characterized by Permian to Miocene formations deposited in shallow to deep basinal environments. The lower part of the succession is represented by the ‘Lagonegro lower sequence’ (e.g. Mostardini & Merlini 1986; Ciarapica *et al.* 1990; Ciarapica & Passeri 2005; Rigo *et al.* 2005) and includes the following formations (from oldest to youngest): Monte Facito Formation (Permian to upper Ladinian); Calcari con Selce (upper Ladinian to Rhaetian); Scisti Silicei (Rhaetian to Tithonian); and Flysch Galestrino (Tithonian to Lower Cretaceous). This lower sequence, always detached from its basement, is dissected into several tectonic units piled up between the Apenninic and Apulian carbonate platforms (e.g. Mostardini & Merlini 1986) during Apenninic orogenesis.

The Upper Triassic–Middle Jurassic Calcari con Selce and Scisti Silicei formations consist of pelagic carbonates and siliceous deposits (i.e. cherts and radiolarites) bearing conodonts, pelagic bivalves (e.g. genus *Halobia*), radiolarians and sparse ammonoids. In proximal palaeogeographical settings, the Calcari con Selce persisted from the Late Triassic to the Early–Middle Jurassic (e.g. Scandone 1967; Bertinelli *et al.* 2005a; Passeri *et al.* 2005), whereas in more distal settings, a transition from carbonate sedimentation of the Calcari con Selce to siliceous deposition of Scisti Silicei occurred between the latest Triassic and the earliest Jurassic and is interpreted as due to the subsidence of the ocean floor below the CCD (e.g. Amodeo 1999; Giordano *et al.* 2010). A precursory switch from carbonate to siliceous deposition is documented during the Carnian (Rigo *et al.* 2007) and is interpreted as due to a transitory shift towards more humid climate conditions (Rigo & Joachimski 2010; Rigo *et al.* 2012a; Trotter *et al.* 2015). Because of the difficulties in placing a boundary between the Calcari con Selce and the Scisti Silicei, Miconnet (1982) first introduced the term ‘Transitional Interval’ to designate the stratigraphical portion of the Lagonegro succession that was included in the upper part of the Calcari con Selce and characterized by an increase of red radiolaritic intercalation, typical of the overlying Scisti Silicei (Amodeo 1999; Bertinelli *et al.* 2005a; Passeri *et al.* 2005; Reggiani *et al.* 2005; Rigo *et al.* 2012b). In particular, the base of the Transitional Interval is conventionally marked by a 2.5- to 4-m-thick interval of red shales (Amodeo 1999; Bertinelli *et al.* 2005b; Reggiani *et al.* 2005; Rigo *et al.* 2012b) of Sevatian 1 age (*Mockina bidentata* Zone – late Norian) (Rigo *et al.* 2005, 2012b). However, in-depth investigations, mostly for biostratigraphy (e.g. De Wever & Miconnet 1985; Bertinelli *et al.* 2005a; Passeri *et al.* 2005; Reggiani *et al.* 2005; Rigo *et al.*

2005, 2012b), revealed that this red shale interval shows atypical features in the Pignola-Abriola section, while it is easily recognized in the Mt. Volturino section.

Pignola-Abriola section: candidate for the Rhaetian GSSP

Lithostratigraphy

The Pignola-Abriola section was measured on the western side of Mt. Crocetta along road SP5 ‘della Sellata’ connecting the villages of Pignola and Abriola (Geographic coordinate system, datum WGS 84: 40° 33′ 23.50″N, 15° 47′ 1.71″E) (Fig. 1). The Pignola-Abriola section is located in an area of minimal structural deformation and within the protected area of the Parco Appennino Lucano Val d’Agri Lagonegrese (Fig. 1).

The section is a ca. 63-m-thick basal succession dominated by the Calcari con Selce and encompassing the Norian/Rhaetian boundary (Amodeo *et al.* 1993; Amodeo 1999; Bazzucchi *et al.* 2005; Rigo *et al.* 2005, 2012b; Giordano *et al.* 2010) (Fig. 2). Thinly bedded cherty limestones (partially dolomitized in the lowermost part of the section) constitute the dominant lithology, sometimes intercalated with centimetre-thick calcarenites due to sporadic gravity flows/turbiditic events (e.g. Amodeo 1999; Bertinelli *et al.* 2005a; Giordano *et al.* 2011). The siliciclastic input increases in the upper part of the Calcari con Selce at the transition with the overlying Scisti Silicei, where shales, radiolarites and subordinate marls dominate. The lower portion of the section (ca. 0–6.5 m) (Fig. 2) consists mainly of well-stratified, thinly bedded cherty dolostones; chert nodules become frequent above ca. 3.5 m. Calcarenites linked to gravity flow events and containing fragments of benthic organisms are subordinate. From ca. 6.5 up to metre 13, repeated intercalations of shales, several centimetres thick, are present. Cherty layers become abundant at ca. 13 m from the base. Between ca. 13 and 22.5 m, limestones gradually replace dolostones and consist mainly of mudstones–wackestones, and less commonly packstones, with abundant radiolarians and rare bivalves. From 22.5 m up to ca. 39 m, shale frequency decreases and centimetre-thick chert bands in limestone beds are common. In addition, three diameter-thick, often amalgamated and partially dolomitized, fining-upward beds of calcarenite occur between ca. 34 and 35.5 m and provide useful lithomarkers (Maron *et al.* 2015). Between 39 and 43.5 m, nodules and especially layers and bands of black radiolarian

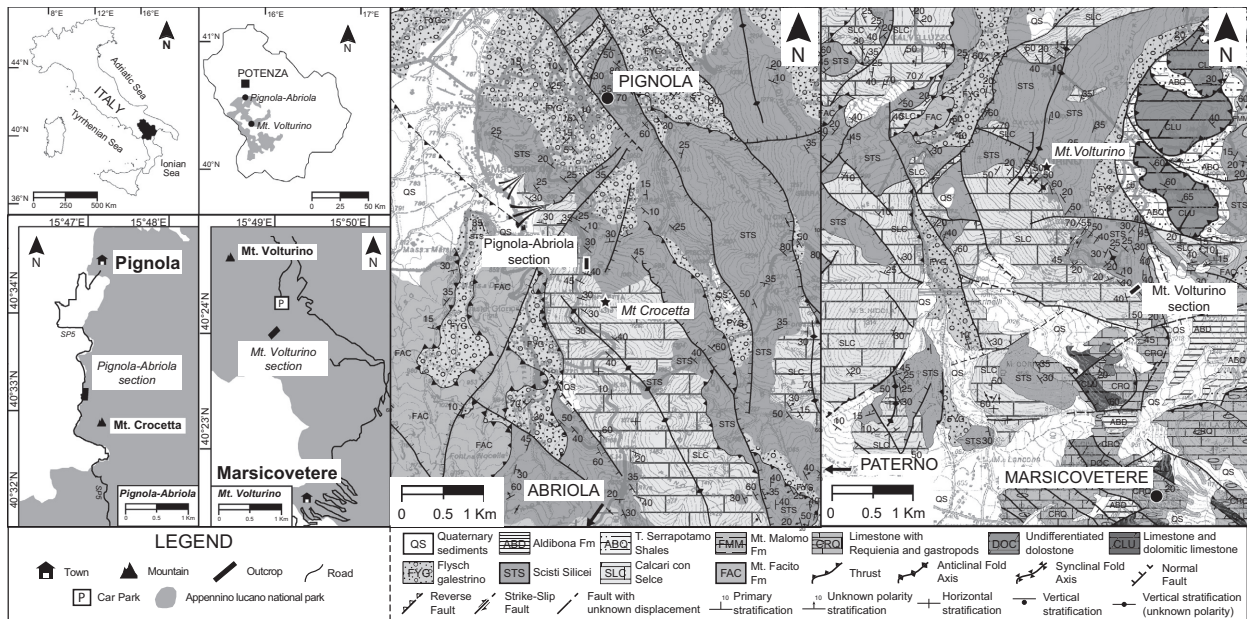


Fig. 1. Geological map (modified from Foglio Geologico 489-Marsico Nuovo and Foglio Geologico 505-Moliterno; <http://www.isprambiente.gov.it/Media/carg/>) and location map of the Pignola-Abriola and Mt. Volturino sections. Both sections crop out in Southern Apennines, near Potenza (Southern Italy), in the protected area of the Parco Appennino Lucano Val d'Agri Lagonegrese. The Pignola-Abriola section crops out along the main road SP 5 'della Sellata', on the western flank of Mt. Crocetta (Lat: 40°33'23,50"N; Long: 15°47'1,71"E). The Mt. Volturino section is exposed close to the homonymous mountain peak, to the north of Marsicovetere village (Lat: 40°24'13,46"N; Long: 15°49'2,25"E).

cherts become abundant, with an increase in terrigenous input up to 56 m. The shales are typically dark and rich in organic matter, often interbedded with silicified limestones and thin calcarenites, deposited in low oxygen (dysoxic to anoxic) conditions. This frequent alternation of shales, limestones, fine-grained calcarenites, marls and chert beds constitute the so-called Transition Interval (Miconnet 1982; Amodeo 1999) separating the Calcarei con Selce from the Scisti Silicei, although at Mt. Crocetta the lower part of Scisti Silicei does not crop out extensively. The uppermost part of the Pignola-Abriola section (ca. m 56–58) is characterized by diameter-thick micritic limestone beds with few clayey intercalations, overlain by red radiolarites and chert layers typical of the Scisti Silicei, extending up to the top of the measured section (at ca. m 63).

Biostratigraphy

The Pignola-Abriola section has been studied in detail for conodonts and radiolaria (Amodeo 1999; Bazzucchi *et al.* 2005; Rigo *et al.* 2005, 2012b; Giordano *et al.* 2010) (Figs 2, 3).

Conodonts are common throughout the entire section, even though they are rare around the NRB, as first noted by Krystyn *et al.* (2007a,b). The Conodont Alteration Index (CAI) is 1.5, suggesting that burial temperatures never exceeded 100 °C (*sensu*

Epstein *et al.* 1977; Bazzucchi *et al.* 2005; Giordano *et al.* 2010; Maron *et al.* 2015). In stratigraphical order, the following updated and main bioevents have been recognized:

- at metre 7, sample PI5, the first occurrence (FO) of *Mockina bidentata*;
- at metre 21.4, sample PR16, FO of *Misikella hernsteini*, co-occurring with *Parvigondolella andrusovi*;
- at metre 32, sample GNC3, the FO of *Misikella buseri*;
- at metre 33.4, sample PR10, the FO of *Misikella hernsteini/posthernsteini* morphocline;
- at metre 44.9, in sample PIG24, the first appearance datum (FAD) of *Misikella posthernsteini* s.s.; and
- at metre 55.5, sample GNC100, the FO of *Misikella ultima* in association with *Misikella koesseensis*.

The radiolarian associations (Figs 2, 4) are well preserved and conform to the biozonation proposed by Carter (1993), which consists of radiolarian assemblage zones biochronologically correlated to the North America ammonoid zonation proposed by Tozer (1979):

- Sample PR14 at metre 25 yielded a radiolarian assemblage referable to the *Betracium deweveri*

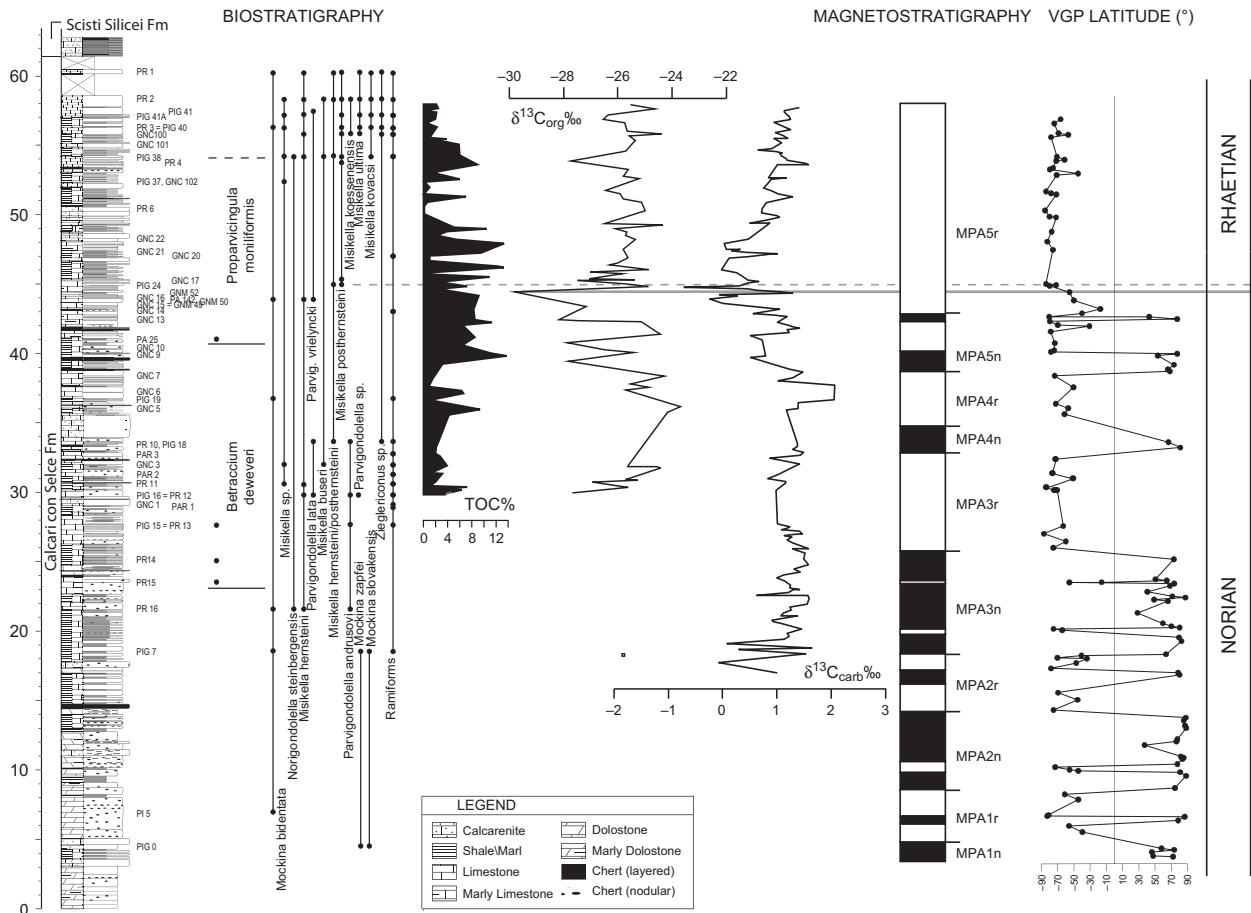


Fig. 2. The Pignola-Abriola section with, from left to right, stratigraphical log, radiolarian and conodont biostratigraphy, total organic matter percentage (TOC), and $\delta^{13}\text{C}_{\text{org}}\text{‰}$ and $\delta^{13}\text{C}_{\text{carb}}\text{‰}$ curves. Magnetostratigraphy and the virtual geomagnetic poles (VGP) are from Maron *et al.* (2015). The prominent $\delta^{13}\text{C}_{\text{org}}\text{‰}$ negative shift located close to the FAD of conodont *Misikella posthernsteini* s.s. is here reported as primary proxy for the base of the Rhaetian. Notably, the $\delta^{13}\text{C}_{\text{org}}\text{‰}$ negative peak occurs within the base of the radiolarian *Proparvicungula moniliformis* Zone.

Zone (U.A. 1 Carter 1993) based on the presence of *Betraccium deweveri* Pessagno & Blome, *Praemesotaturnalis gracilis* Kozur & Mostler, *Tetraporobrachia* sp. aff. *T. composita* Carter, *Ayrtonius elizabethae* Sugiyama, *Citriduma* sp. *A sensu* Carter (1993), *Globolaxtorum* sp. cf. *G. hullae* (Yeh & Cheng), *Lysemela* sp. cf. *L. olbia* Sugiyama, *Livarella valida* Yoshida and *Livarella* sp. *sensu* Carter (1993) (Giordano *et al.* 2010); a similar assemblage was found also in sample PR15 at metre 23.5 and sample PR13 at metre 27.5. The presence of *Globolaxtorum* sp. cf. *G. hullae* Yeh & Cheng in this assemblage is atypical, because the genus *Globolaxtorum* is usually referred only to the *Proparvicungula moniliformis* and *Globolaxtorum tozeri* zones (O'Dogherty *et al.* 2009).

- Sample PA25 at metre 41 yielded a radiolarian assemblage referable to the *Proparvicungula moniliformis* Zone, Assemblage 1 and 2, Subassemblage

2a (U.A. 2–8 Carter 1993), for the presence of *Fontinella primitiva* Carter, *Praemesotaturnalis* sp. cf. *P. sandspitensis* Blome, *Globolaxtorum* sp. cf. *G. hullae* Yeh & Cheng and *Livarella densiporata* Kozur & Mostler (Bazzucchi *et al.* 2005; Giordano *et al.* 2010).

Misikella posthernsteini is a phylogenetic descendent of *M. hernsteini* (e.g. Mostler *et al.* 1978; Kozur & Mock 1991; Giordano *et al.* 2010). Both species display a similar cusp as posterior denticle, but they differ in (1) number of blade denticles, which are 3 (rarely 4) in *M. posthernsteini* and 4–6 in *M. hernsteini*; and (2) shape of the basal cavity, which is shaped like a heart or drop in *M. posthernsteini* and *M. hernsteini*, respectively. All specimens with intermediate features are grouped in the *Misikella hernsteini/posthernsteini* morphoclines and are here referred to as *Misikella hernsteini/posthernsteini* transitional forms; they are characterized by

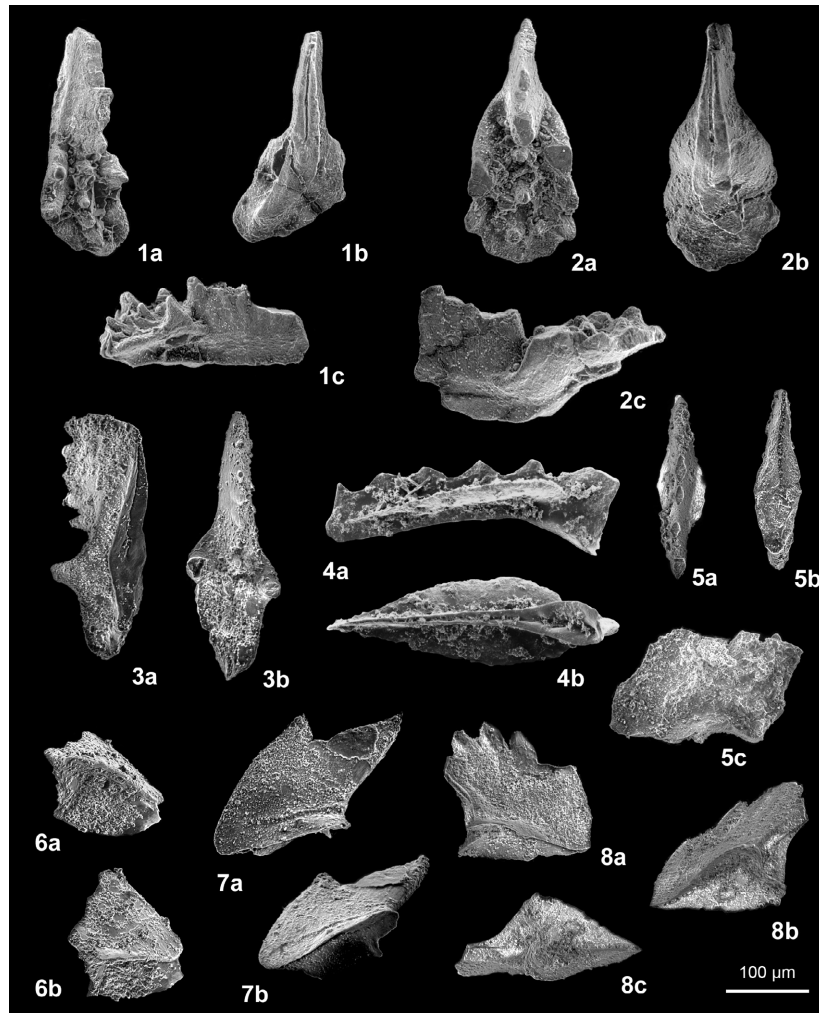


Fig. 3. SEM micrographs of upper Norian to Rhaetian conodonts from the Pignola-Abriola section Calcari con Selce Fm (after Bazzucchi *et al.* 2005 and Giordano *et al.* 2010, modified). Scale bar = 100 μm . 1, a, b, c, *Mockina zapfei* (Kozur); sample PIG 0. 2, a, b, c, *Mockina slovakensis* (Kozur); sample PIG 0. 3, a, b, *Mockina bidentata* (Mosher); PIG 7. 4, a, b, *Norigondolella steinbergensis* (Mosher); PR 16. 5, a, b, c, *Misikella hernsteini* (Mostler); sample PIG 16. 6, a, b, *Misikella posthernsteini* Kozur & Mock; sample PIG 24. 7, a, b, *Misikella kovacsi* Orchard; sample PIG 40. 8, a, b, c, *Misikella ultima* Kozur & Mock; sample PIG 40.

the reduction of the number of blade denticles and the evolution of the drop-shaped basal cavity into a heart shape. These transitional forms are also well documented in other sections of the Lagonegro Basin (e.g. Giordano *et al.* 2010), as well as the Lombardian Basin of northern Italy (Muttoni *et al.* 2010). The occurrence of the *Misikella hernsteini/posthernsteini* morphoclines is followed by the occurrence of *Misikella posthernsteini sensu stricto* (m 44.9, sample PIG24), providing a continuous and reliable biostratigraphical signal (Remane 2003). Calibration with radiolarian biostratigraphy (Giordano *et al.* 2010) reveals that only those specimens of *Misikella posthernsteini* characterized by a heart-shaped basal cavity due to a real groove on the posterior margin of the basal cavity developed by the extension of a distinct furrow along the backside of the cusp occurred within the radiolar-

ian *Proparvicungula moniliformis* Zone (*sensu* Carter 1993). These specimens were interpreted as *Misikella posthernsteini sensu stricto* (Giordano *et al.* 2010).

Recently, calcareous nannofossils (e.g. *Prinsiosphaera* sp.) also were recorded and estimated to contribute between 2.5 and 15% to the amount of carbonate production at the Pignola-Abriola section (Preto *et al.* 2013).

Notably, thin cross-section bivalve shells have been observed in the limestone beds of the Pignola-Abriola section, but no good specimens have been collected from these strata. However, a single specimen of *Monotis limaeformis* Gemmellaro was documented in the Mt. Sirino area (De Lorenzo 1894), ca. 50 km to the south of the Pignola-Abriola section. This species is strictly related to the *Monotis salinaria* group (De Lorenzo 1894; Grant-Mackie

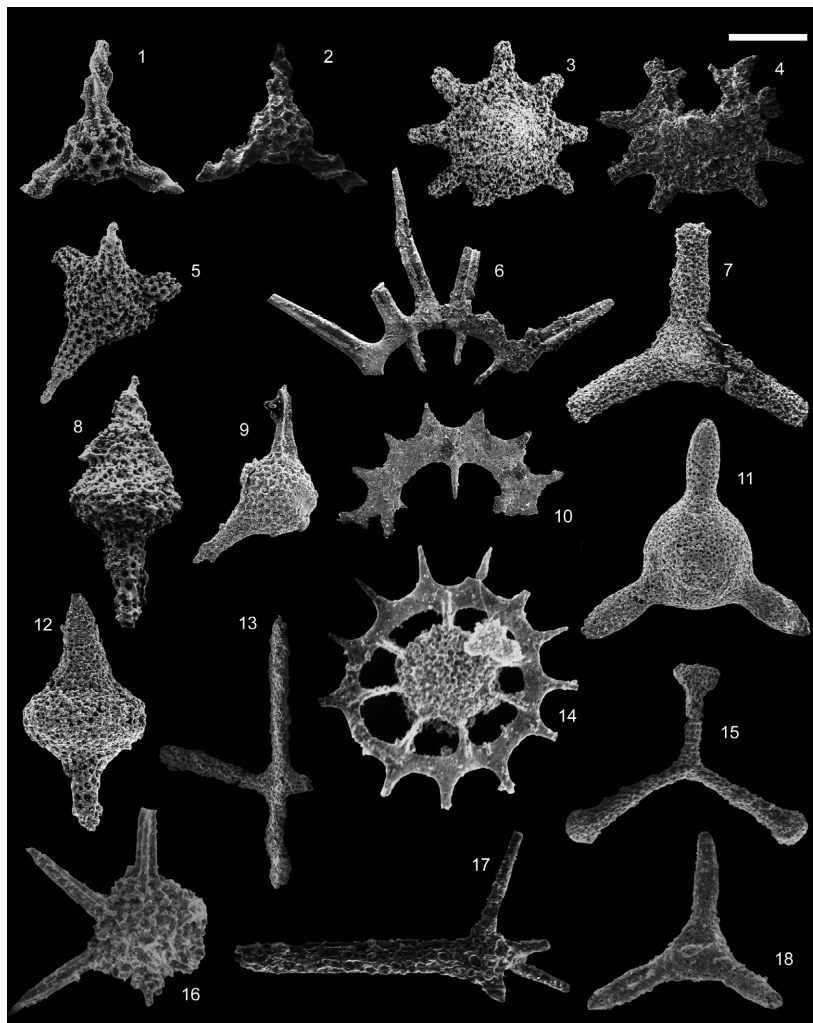


Fig. 4. Upper Norian–Rhaetian radiolarians from the Calcarei con Selce (Pignola-Aabriola section) and from the Scisti Silicei (Mt. Volturino section). Samples PR13, PR14 and PR15 from Pignola-Aabriola, and sample MVV5 from Mt. Volturino, are referred to the *Betraccium deweveri* Zone; sample PA25 (Pignola-Aabriola) is referred to the *Proparvicingula moniliformis* Zone, Assemblage 1; sample MV23 (Mt. Volturino) is referred to the *Proparvicingula moniliformis* Zone, Assemblage 1–2 and MV 31 (Mt. Volturino) to the *Globolaxtorum tozeri* Zone Assemblage 3. Scale bar = 100 μm for 1–2, 8–12, 14–15; 150 μm for 6; 200 μm for 3–5, 7, 16–18 (after Bazzucchi *et al.* 2005 and Giordano *et al.* 2010, 2011, modified). 1. *Betraccium deweveri* Pessagno & Blome, sample PR14. 2. *Betraccium deweveri* Pessagno & Blome, sample PR14. 3. *Citriduma* sp. A, *sensu* Carter (1993), sample PR13. 4. *Citriduma* sp. A, *sensu* Carter (1993), sample MVV5. 5. *Tetraporobrachia* sp. aff. *T. composita* Carter, sample PR14. 6. *Praemesosaturnalis gracilis* (Kozur & Mostler), sample PR14. 7. *Livarella* sp., *sensu* Carter (1993), sample PR14. 8. *Globolaxtorum* sp. cf. *G. hullae* (Yeh & Cheng), sample PR14. 9. *Fontinella primitiva* Carter, sample PA 25. 10. *Praemesosaturnalis* sp. cf. *P. sandspitensis* (Blome), sample PA25. 11. *Livarella densiporata* Kozur & Mostler, sample PA25. 12. *Globolaxtorum hullae* (Yeh & Cheng), sample PA25. 13. *Pseudohagiastrum* sp. A *sensu* Carter 1993, sample MV23. 14. *Praemesosaturnalis* sp. aff. *P. sandspitensis* (Blome), sample MV31. 15. *Paronaella pacofiensis* Carter, sample MV23. 16. *Octostella dihexacanthus* (Carter), sample MV31. 17. *Pseudohagiastrum giganteum* Carter & Hori, sample MV 31. 18. *Livarella valida* Yoshida, sample MV31

1978), which is Sevastian in age (late Norian) (e.g. McRoberts 2010).

Chemostratigraphy

The Pignola-Aabriola section has been investigated for organic carbon isotope ($\delta^{13}\text{C}_{\text{org}}$) and total organic carbon (TOC) variations. Rock samples were collected from the section (76 samples) (Table 1), washed in millipore water and selected to avoid the sampling of not representative portions of

the sample (e.g. fracture-filling mineralization, bioturbation, diagenetic alterations). Several grams of each sample (<5 g) were reduced to a fine powder using a Retsch RM0 grinder and dried overnight at 40 °C.

The TOC investigations were conducted following the standard acid attack method (Schlanger & Jenkyns 1976), which requires the reaction of the powders with a 10% HCl solution in silver capsules. Once the reaction was finished, the samples were dried on a hot plate at 50 °C. All samples were anal-

ysed using a Vario Macro CNS Elementar Analyser at the University of Padova. Results were calibrated against Sulphanilamide standard (N = 16.25%; C = 41.81%; S = 18.62%; H = 4.65%). The analytical uncertainty of the instrument is $\sigma = 0.5\%$ (% RSD, relative standard deviation).

For the $\delta^{13}\text{C}_{\text{org}}$ measurements, pulverized rock samples were acid-washed with 10% HCl for at least three hours (usually overnight). Successively, the samples were neutralized in millipore water, dried at 40 °C overnight and wrapped in tin capsules. Forty-one samples were analysed using a GVI Isoprime CF-IRMS mass spectrometer at Rutgers University: multiple blank capsules and isotope standards (NBS 22 = -30.03% ; Coplen *et al.* 2006; and an in-house standard) were added for every batch of isotopic analysis. The standard deviation of the in-house standards during the period of analyses was better than 0.2% . Fifteen samples were analysed using a Delta V Advantage mass spectrometer connected to a Flash HT Elementar Analyser at the University of Padova. For every set of analysis, multiple blank capsules and isotope standards (IAEA CH-6 = -10.45% , IAEA CH-7 = -32.15% , Coplen *et al.* 2006) were included. The standard deviation of the in-house standard during the period of analyses was better than $\sigma = 0.3\%$.

$\delta^{13}\text{C}_{\text{org}}$ and $\delta^{13}\text{C}_{\text{carb}}$ profiles. – The recorded $\delta^{13}\text{C}_{\text{org}}$ shows a minimum of -29.95% and a maximum of -23.70% , with an average value of ca. -25.95% . Between metre 36 and 44.4, the curve depicts an important negative shift, with amplitude of ca. 6% , over a span where the TOC content roughly doubled (Fig. 2). This shift exhibits a marked negative peak at metre 44.4 m ($\delta^{13}\text{C}_{\text{org}} = -29.95\%$, highlighted by the grey line in Fig. 2), ca. 50 cm below and thus almost coincident with the FAD of the conodont *Misikella posthernsteini* s.s. (dashed line in Fig. 2; Maron *et al.* 2015) and 4 m above the beginning of the radiolarian *Proparvicungula moniliformis* Zone, Assemblage 1 (*sensu* Carter 1993; Giordano *et al.* 2010) (Fig. 2). Because it is relatively easy to recognize and has good potential for global correlation, we propose the lowest $\delta^{13}\text{C}_{\text{org}}$ value close to the FAD of *M. posthernsteini* s.s., within the *P. moniliformis* Zone (*sensu* Carter 1993; Giordano *et al.* 2010), as a geochemical marker for the GSSP of the Rhaetian (Fig. 2). This negative peak occurs during a $\delta^{13}\text{C}_{\text{org}}$ short-term excursion, which falls within a longer term decrease of the $\delta^{13}\text{C}_{\text{org}}$.

The stable isotope composition of carbonate ($\delta^{13}\text{C}_{\text{carb}}$) ranges from $-1.80 \pm 1.00\%$ to $2.07 \pm 1.00\%$, with a mean of ca. $0.99 \pm 1.00\%$ (Preto *et al.* 2013). Around the NRB, the $\delta^{13}\text{C}_{\text{carb}}$

curve follows almost perfectly the trend of the $\delta^{13}\text{C}_{\text{org}}$ curve, showing a significant negative shift at ca. 45 m ($\delta^{13}\text{C}_{\text{carb}} = -0.69 \pm 1.00\%$), almost coincident with the FAD of the *M. posthernsteini* (Fig. 2).

The close parallelism between the $\delta^{13}\text{C}_{\text{org}}$ and $\delta^{13}\text{C}_{\text{carb}}$ confirms that the Pignola-Abriola isotopic signal is primary. Decreasing trends in both curves are regarded as due to an input of isotopically light carbon in the ocean system, which may be linked to decrease in primary productivity, decrease in organic carbon burial, clathrates dissociation, wildfires, isolation of epicontinental seas and/or emplacement of large igneous provinces (LIPs) (e.g. Hesselbo *et al.* 2002; Higgins & Schrag 2006; Jenkyns 2010; Tanner 2010; Meyer 2014).

Magnetostratigraphy

A total of 220 samples have been collected for palaeomagnetic analyses and 9 for rock magnetism experiments (IRM). The analyses were performed at the Alpine Laboratory of Paleomagnetism (ALP) of Peveragno, Italy. The samples were thermally demagnetized up to 675 °C and then analysed with a 2G three-axial DC-SQUID cryogenic magnetometer. For details, see Maron *et al.* (2015).

The analysis of the NRM indicates a mean magnetization of the samples of 0.08 mA/m. Rock magnetic experiments indicate haematite and magnetite as the main carriers of the magnetization, with subsidiary iron sulphide (Maron *et al.* 2015). The characteristic component of magnetization (ChRM) was isolated in 121 samples (ca. 55%) mainly up to 450–550° (maximum of 625 °C), showing north-down and south-up directions. The reversal test of McFadden & McElhinny (1990) was applied to the ChRM component directions and resulted positive (Maron *et al.* 2015). A sequence of virtual geomagnetic poles (VGPs) was obtained from the ChRM directions. The VGP latitudes have been arranged in stratigraphical order to obtain a sequence of geomagnetic polarity reversals along the Pignola-Abriola section. A total of 22 polarity reversals have been recognized and grouped in 10 magnetozones labelled from MPA1n to MPA5r (Fig. 2).

The Pignola-Abriola section was then correlated to Tethyan sections from the literature provided with magnetostratigraphy and conodont biostratigraphy (Fig. 5). The magnetostratigraphy of the Steinbergkogel section (Hüsing *et al.* 2011), GSSP candidate for the Rhaetian stage (Krystyn *et al.* 2007a,b; Krystyn 2008), is comparable with the data from Pignola-Abriola, only introducing a revision in the biostratigraphy of Steinbergkogel. We think that

Table 1. Stable isotope composition of carbon ($\delta^{13}\text{C}_{\text{org}}$) and percentage of organic matter (TOC) versus sample height position of the Pignola-Abriola and Mt. Volturino sections.

PIGNOLA-ABRIOLA				MT. VOLTURINO			
m	Sample	TOC%	d13Corg	m	Sample	TOC%	d13Corg
58.10	Pa i 191	1.984		71.00	MV49	0.611	-19.88
57.80	Pai 189	2.321	-25.56	68.00	MV45.60	0.115	
57.65	GNM 119	0.149		66.00	MV44	0.161	-21.89
57.50	Pai 187	2.014	-24.66	65.00	MV 43	0.174	-25.15
57.05	Pai 185	1.863	-26.43	64.00	MV42	0.294	
56.76	GNM 117	0.452	-26.61	57.50	MMV 9	0.095	
56.50	Pai 184	2.103	-25.80	56.00	MVV8	0.371	
55.70	GNI 29	0.960	-24.41	52.00	MMV 1	0.693	-28.05
55.63	Pai 180	3.654	-25.71	51.50	MV 35	0.380	
55.55	GNI 28	1.259	-25.63	51.00	MMV 2	1.111	-27.78
55.25	GNI 27	5.548	-25.40	50.66	MMV 3		-27.36
54.45	Pai 173	5.663	-25.77	50.50	MMV 4	0.941	-26.33
53.75	GNM 102	8.410	-27.83	49.50	MMV 6	0.925	-26.56
53.15	Pai 168	1.359	-25.67	49.00	MMV 7	1.192	-27.52
52.65	GNI 26	5.684	-25.85	48.20	MMV 8		-25.23
52.50	Pai 166	0.136	-25.26	47.10	MMV 9		-27.46
52.13	Pa i 164	0.963		46.60	MMV 10		-26.50
51.65	Pai 162	0.079	-26.52	46.50	MV 31	0.124	
51.40	GNI 25	6.664	-25.97	46.20	MMV 11		-25.42
51.05	GNM 85	0.618	-25.86	45.00	MVV 6	0.706	
50.80	Pai 160	0.096	-25.17	42.50	MV 27B	0.288	-23.47
50.20	Pai 157	0.107	-25.03	42.45	MMV 13		-27.35
49.25	GNI 24	4.780	-26.56	41.50	MV 24	0.195	-24.29
49.15	GNI 23	9.895	-24.36	41.43	MMV 16		-24.25
48.90	GNI 22	3.667	-26.15	41.00	MV 23	0.295	-26.13
48.65	Pai 155	2.113	-25.72	40.20	MV 22		-26.12
48.40	GNI 21	5.074	-25.77	39.50	MV 21	0.198	
48.10	GNI 20	12.653	-25.40	39.00	MV 20B	0.384	
47.40	GNI 19B	9.024	-25.86	38.45	MMV 22		-24.73
47.20	Pa i 146 Dark	1.895		38.00	MMV 23		-24.67
47.20	Pa i 146 Bright	0.945		38.00	MV 17	0.293	-26.07
46.80	GNI 19	0.943	-25.68	37.50	MV 16	0.500	-23.15
46.45	GNI 18	11.623	-26.05	36.30	MMV 27		-24.30
46.30	GNI 17	12.589	-26.37	37.00	MV15	0.479	
45.95	Pai 143	0.106	-24.90	36.00	MVV 5	0.329	-24.52
45.80	GNI 16	0.728	-27.10	35.60	MMV 29		-24.35
45.65	Pai 142	10.337	-25.89	35.00	MV11	1.092	-24.86
45.30	GNI 15	2.032	-27.13	34.00	MVC7	0.310	-23.65
45.23	GNI 14	2.566	-25.42	34.00	MMV 32	0.389	
45.18	Pai 139		-27.58	33.50	MMV 33	0.891	
44.95	Pai 136	6.856	-25.80	32.00	MVV4	0.367	
44.75	Pai 134	2.321	-24.91	31.00	MVC6	0.215	-25.60
44.35	GNM 52	8.663	-29.95	30.50	MV7	0.323	-24.83
43.30	GNP 3	7.845	-27.26	29.00	MVC 5	0.218	-26.29
42.60	Pa i 119	8.045					
42.35	GNP 2	10.681	-28.28				
42.28	GNM 41A	8.327	-27.55				
42.20	Pai 116	6.125	-25.18				
41.30	Pai 111	8.014	-24.46				
40.70	GNM 37	6.074	-27.97				
40.19	GNM 35B	10.557	-26.55				
40.00	Pai 108	13.025	-25.47				
39.35	GNP 1	2.967	-27.93				
38.30	Pai 104	1.451	-24.31				
37.73	GNI 13	0.818	-25.58				
37.50	GNI 12	5.960	-24.90				
37.30	GNI 11	6.261	-25.76				
36.80	Pai 101	0.941					
36.10	GNI 10	8.876	-23.70				
35.70	GNI 9	3.992	-24.19				
33.80	Parc 1	2.354					
33.40	Parc 3	1.979	-25.97				
32.95	Parc 6	1.853					

(continued)

Table 1. (Continued)

PIGNOLA-ABRIOLA				MT. VOLTURINO			
m	Sample	TOC%	d13Corg	m	Sample	TOC%	d13Corg
32.70	Parc 7	2.580					
32.05	Parc 10	3.668					
31.70	GNI 8	1.855					
31.65	GNI 7	0.309	-24.58				
31.60	GNI 6	0.164					
31.50	Parc 12	2.923	-25.96				
30.89	Parc 15	1.880					
30.70	GNI 5	1.348					
30.65	GNI 4	0.152	-25.30				
30.55	GNI 3	6.841	-26.95				
30.40	Parc 16	2.036					
30.30	GNI 2	5.996	-25.66				
29.90	GNI 1	2.589	-27.68				

the first occurrence (FO) of conodont *Misikella posthernsteini* at Steinbergkogel (see specimens in plate 1 in Krystyn *et al.* 2007a) should be considered equivalent to the FO of *Misikella hernsteini/posthernsteini* transitional forms (*sensu* Giordano *et al.* 2010) in the Pignola-Abriola section (Maron *et al.* 2015). In particular, the main reversal interval in Steinbergkogel (ST1/B- to ST1/H- in STK-A subsection; ST2/B- to ST2/H- in STK-B+C subsection) is considered equivalent to magnetozone from MPA3r to MPA5r at Pignola-Abriola (Fig. 5). In addition, we find that the Norian/Rhaetian Oyuklu section (Gallet *et al.* 2007) is comparable with Pignola-Abriola whereby interval from Oyuklu magnetozone OyB- to OyD- should correspond to magnetozone MPA4r to MPA5r at Pignola-Abriola (Fig. 5). Moreover, the upper part of the Carnian–Norian Pizzo Mondello section (Muttoni *et al.* 2004), from magnetozone PM-8n to PM-12n, should correspond to the lower part of the Pignola-Abriola section from MPA1n to MPA3n, equivalent to the magnetozone SB-8n to SB-11n in the Silická Brezová section (Channell *et al.* 2003) (Fig. 5). Notably, conodont biostratigraphy of Silická Brezová section has been reclassified after Mazza *et al.* (2012). The Pignola-Abriola section also has been correlated with the Brumano/Italcementi Quarry composite section, upper Rhaetian to Hettangian in age (Muttoni *et al.* 2010, 2014), using as tie point the FO of *M. posthernsteini* s.s. We conclude that the magnetostratigraphy of the Brumano/Italcementi Quarry section is substantially younger than the magnetostratigraphy of Pignola-Abriola.

Prospects for high-precision geochronology. – Sedimentation rates were estimated by comparing the thickness of the Pignola-Abriola magnetozone with the duration of their equivalent magnetozone in the Newark APTS (Olsen *et al.* 2011)

(Fig. 6). The resulting preferred correlation option implies depositional rates that are very low (ca. 2.6 m/My) in the lower portion of the section (from the base to ca. 26 m), increasing to ca. 5.6 m/My from metre 26, and reaching ca. 9.8 m/My from metre 43.5 upwards (Maron *et al.* 2015). The presence of more marls, shales and marly limestones in the upper part of the section suggests a major input of siliciclastic fraction, consistent with the observed increase of sedimentation rates and the higher concentration of magnetic minerals. The age model derived from this preferred correlation option was used to date the level containing the Norian/Rhaetian boundary (approximated by the carbon isotope shift and associated bioevents; see above) to ca. 205.7 Ma (see Maron *et al.* 2015 for details), in substantial agreement with the high-precision U-Pb geochronology constraints by Wotzlaw *et al.* (2014). Considering a Triassic/Jurassic boundary at 201.3 Ma (Schoene *et al.* 2010; Guex *et al.* 2012), the Rhaetian is ca. 4.4 Myr long; considering the Carnian/Norian boundary at ca. 227 Ma (Muttoni *et al.* 2004; Maron *et al.* 2015), the Norian Stage is ca. 21.3 Myr long.

Age of the main events around the Norian/Rhaetian boundary. – The calibration of the Pignola-Abriola magnetostratigraphy with the Newark APTS (Olsen *et al.* 2011) allows dating the main events recorded around the Norian/Rhaetian boundary. For instance, the Sevatian1/Sevatian2 boundary, defined by the FO of conodont *Misikella hernsteini*, is placed at ca. 210.8 Ma, while the FO of *Mockina bidentata* (Alaunian/Sevatian boundary) is at ca. 216.2 Ma (Fig. 6). The FO of the *M. hernsteini/posthernsteini* transitional morphotype, corresponding to the older *Misikella posthernsteini* specimens *sensu* Krystyn *et al.* (2007a), is placed at ca. 207.6 Ma (Fig. 6). The FO

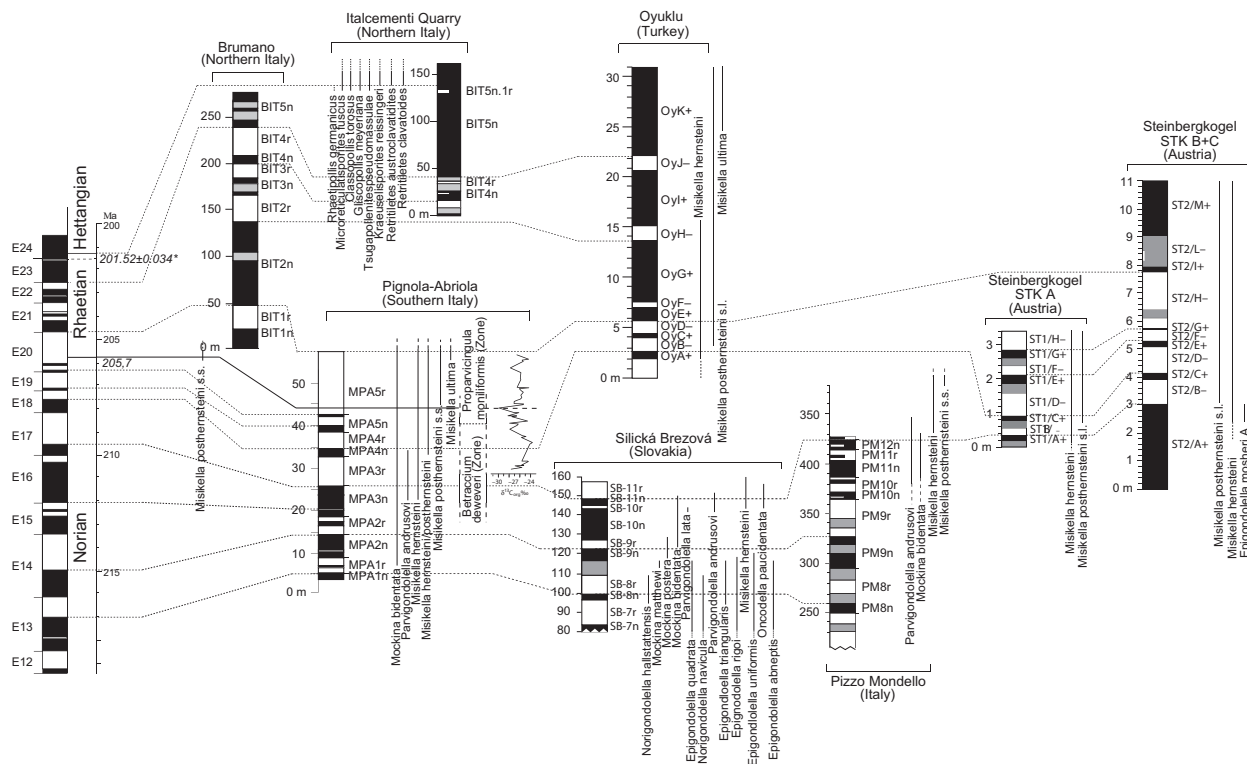


Fig. 5. Correlation of the magnetostratigraphy and biostratigraphy of the Pignola-Abriola section with data from Tethyan marine sections in literature, as Steinbergkogel (STK-A and B+C; Hüsing *et al.* 2011), current GSSP candidate for the Rhaetian Stage (Krystyn *et al.* 2007a,b), Brumano/Italcementi Quarry (Muttoni *et al.* 2010, 2014), Oyuklu (Gallet *et al.* 2007), Pizzo Mondello (Muttoni *et al.* 2004, 2014) and Silická Brezová (Channell *et al.* 2003). Conodont biostratigraphy of Silická Brezová reclassified after Mazza *et al.* (2012); the specimens of conodont *Misikella posthernsteini* in Steinbergkogel (as considered in Krystyn *et al.* 2007a,b) are here attributed to the *Misikella hernsteini/posthernsteini* transitional form (after Giordano *et al.* 2010). The Pignola-Abriola section is correlated to the Newark Astrochronological Polarity Time Scale (APTS; Olsen *et al.* 2011) following the correlation of Maron *et al.* (2015). The level containing the Norian/Rhaetian boundary in Pignola-Abriola, placed with a negative $\delta^{13}\text{C}_{\text{org}}$ spike of ca. -30‰ and virtually coincident with the first appearance datum (FAD) of conodont *M. posthernsteini* s.s., is dated at 205.7 Ma (Maron *et al.* 2015), within magnetozone E20r of the Newark APTS.

of *Misikella ultima* is at ca. 204.7 Ma, while the base of the *Proparvicungula moniliformis* Zone (proxy for the NRB) is placed at ca. 206.2 Ma. Finally, the age of the prominent $\delta^{13}\text{C}_{\text{org}}$ negative spike located only 50 cm below the FAD of *M. posthernsteini* s.s. is of ca. 205.7 Ma (Fig. 6).

Demonstration of regional and global correlation

Regional correlation

The litho- and biostratigraphical correlations of the NRB interval in the Lagonegro Basin were well illustrated and discussed by several authors since the end of the 19th century, such as De Lorenzo (1894), Scandone (1967), De Capoa (1970, 1984), Miconnet (1982), Amodeo (1999), Bertinelli *et al.* (2005), Baz-zucchi *et al.* (2005), Reggiani *et al.* (2005), Rigo *et al.* (2005, 2012b) and Giordano *et al.* (2010, 2011). From a biostratigraphical perspective in dif-

ferent localities and sections from the Lagonegro Basin, a well-defined NRB has been documented with the occurrence of the *Misikella posthernsteini* s.s., such as in the Mt. S. Enoc, Pignola-Abriola and Sasso di Castalda sections (e.g. Giordano *et al.* 2010).

We thus studied a second key stratigraphical section, known as Mt. Volturino, which is coeval to the GSSP candidate Pignola-Abriola section but deposited in a deeper depositional setting of the Lagonegro Basin, below the CCD (Giordano *et al.* 2010, 2011). The Mt. Volturino section exposed ca. 17 km to the south of Pignola-Abriola and yielded conodont and radiolarian biostratigraphy as well as a strong $\delta^{13}\text{C}_{\text{org}}$ peak around the NRB (Fig. 7).

The litho-, bio- and chemostratigraphy of the Mt. Volturino section is described hereafter.

Monte Volturino section

Lithostratigraphy. – The section is located along the southern slope of Mt. Volturino (between La Torre and Coste Roberto) (Geographical coordinate

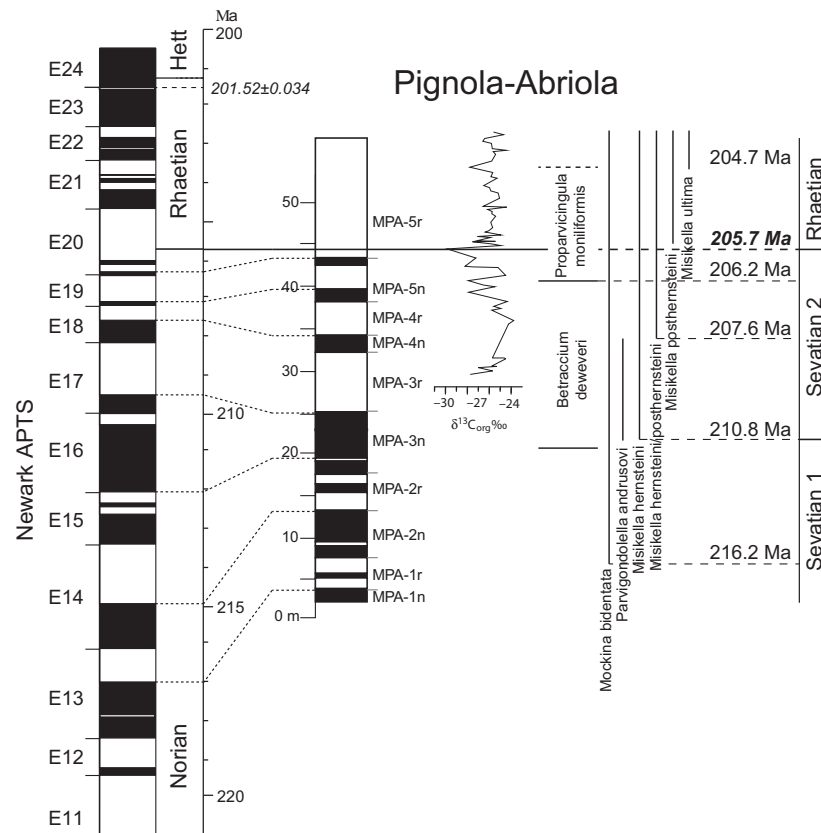


Fig. 6. Litho- and magnetostratigraphical correlations between the Pignola-Abriola section and the Newark APTS based on Maron *et al.* (2015). Chemostratigraphy and biostratigraphy are reported on the right. Calibrated ages of the main bioevents are referred to the age model after Maron *et al.* (2015).

system, datum WGS 84: 40°24'13.46"N; 15°49'2.25"E) within the area of the Parco Appennino Lucano Val d'Agri Lagonegrese, the same protected area of the Pignola-Abriola section (Fig. 1). The Mt. Volturino section shows a very good exposure of the Calcarei con Selce in transition with the overlying Scisti Silicei. The lower 4 metres of the section is represented by cherty limestones (mostly mudstone and wackestones) ascribed to the Calcarei con Selce. At 4 m above the base of the section, a 4-m-thick unit of red shales marks the base of the 'Transitional Interval' (i.e. upper part of Calcarei con Selce) (Fig. 7). Above this horizon, a portion of ca. 9.70 m is characterized by thin red shale layers intercalated to thick cherty limestones beds. The overlying 8.30 m consists instead of thicker red shale layers with thinner cherty limestones intercalations. At 26 m above the base of the section, a 1-m-thick layer of red shales occurs, overlain by an interval rich in shales and silicified limestones characterized by 7 m of very thin cherty limestones (often silicified) alternating with red shales, red cherts and radiolarites (Fig. 7). Within the upper part of the 'Transitional Interval', between 28.70 and 38.0 m, thin dark shales and cherty layers, radiolarites and partially silicified

laminated limestones become dominant and are capped by 1 m of dark shales. Above this organic-rich interval, only siliceous sedimentation occurs, dominated by radiolarites, representing the base of the Buccaglione member of the Scisti Silicei. The basal 12 m of the Buccaglione member consists of red radiolarites, radiolarian cherts and siliceous shales, overlain by a 3-m-thick graded calciruditic bed at 47 m. A 1-m-thick transitional bed characterized by thin calcarenites intercalated with green to red shales is overlain by the Nevéra member of the Scisti Silicei, which consists in black siliceous shales interbedded with silicified calcarenites rich in organic matter (Fig. 7).

Biostratigraphy. – The Mt. Volturino section yielded pyritized radiolarians, in particular in the Transitional interval, and conodont associations in the calcareous portion of the section (e.g. Giordano *et al.* 2010, 2011). The biozonations are those proposed by Kozur (2003) and Carter (1993) for conodont and radiolarian biostratigraphy, respectively. Conodont CAI is 2.5–3 (*sensu* Epstein *et al.* 1977).

Mockina bidentata, *Parvigondolella lata* and *Parvigondolella andrusovi* first occur at ca. 12 m

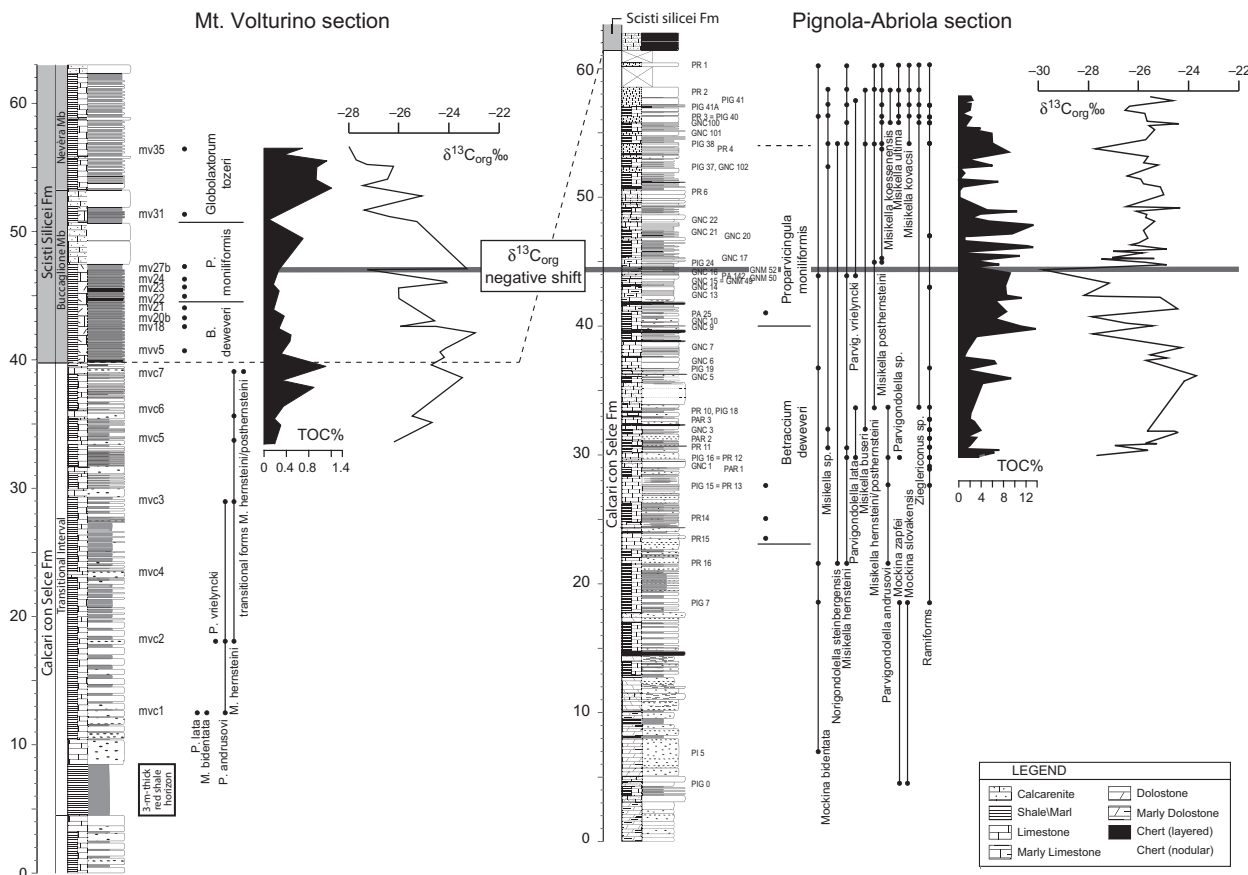


Fig. 7. Stratigraphical log, radiolarian and conodont biostratigraphy of the Mt. Volturino section. Total organic matter percentage (TOC) and $\delta^{13}\text{C}_{\text{org}}$ are compared to the $\delta^{13}\text{C}_{\text{org}}$ curve of the Pignola-Aabriola section, emphasizing the prominent negative shift that is present in both sections and used to define the NRB.

(Giordano *et al.* 2010, 2011), defining the base of the *Mockina bidentata* Zone (Kozur & Mock 1991) (Figs 3, 7). *Misikella hernsteini* first occurs at 18 m, along with *Parvigondolella vrielyncki*, followed by the first occurrence of the *Misikella hernsteini*/*M. posthernsteini* transitional form at 39 m (Giordano *et al.* 2010, 2011) (Figs 3, 7).

From the base of the Scisti Silicei at ca. 39.7 m up to metre 44.5, well-preserved radiolarian assemblages documented the upper Norian *Betraccium deweveri* Zone (U.A. 1 Carter 1993), in particular by the presence of *Citriduma* sp. A, *sensu* Carter (1993) and *Betraccium deweveri* Pessagno & Blome in sample MVV5 (Giordano *et al.* 2010, 2011) (Figs 4, 7). Between metres 44.5 and 51.5, the conjunct occurrence of *Paraonella pacofiensis* Carter and *Pseudohagiastrium* sp. A (*sensu* Carter 1993) can be referred to the *Proparvicungula moniliformis* Zone, in particular to the Unitary Association 5–18 (*sensu* Carter 1993), which corresponds to the upper part of the Assemblage 1 and the lower-mid part of Assemblage 2 (=2a, 2b, 2c) of the *Proparvicungula moniliformis* Zone (Carter 1993). Sample MV 31 at 51.5 m, with

Pseudohagiastrium giganteum Carter & Hori, *Praemososaturnalis* sp. aff. *P. sandspitensis* (Blome), *Livarella valida* Yoshida, *Octostella dihexacanthus* (Carter), is referable to the *Globolaxtorum tozeri* Zone, Assemblage 3 (U.A. 24–27) (Giordano *et al.* 2010, 2011) (Figs 4, 7). Notably, in sample MV27b, *Serilla* sp. aff. *S. tledoensis* is referable to the Unitary Association 16–27 (Carter 1993), which corresponds to the middle-*Proparvicungula moniliformis* Zone (Subassemblage 2c, 2d) and *Globolaxtorum tozeri* Zone (Assemblage 3) (Fig. 7).

Chemostratigraphy. – The Mt. Volturino section has been studied for its $\delta^{13}\text{C}_{\text{org}}$ and TOC composition. Forty-four samples were analysed following the methods described above. The $\delta^{13}\text{C}_{\text{org}}$ values range between a minimum of -28.05‰ and a maximum of -23.15‰ , with an average value of ca. -25.60‰ (Fig. 7; Table 1). The curve displays a main negative shift at m 47 with amplitude in the order of ca. 3‰ . This negative shift likely corresponds to the Pignola-Aabriola negative peak that occurs at 44.4 m ($\delta^{13}\text{C}_{\text{org}} = -29.95\text{‰}$), almost coincident with the

FAD of the conodont *M. posthernsteini* s.s. in the Pignola-Abriola section. Unfortunately, the conodont *M. posthernsteini* was not recovered in the Mt. Volturino section. Nevertheless, the Mt. Volturino and the Pignola-Abriola negative fluctuations both occur in the *Proparvicingula moniliformis* Zone (*sensu* Carter 1993; Giordano *et al.* 2010) (Fig. 7).

Long distance and global correlation. – The succession of conodont and radiolarian faunas in the both Pignola-Abriola and Mt. Volturino sections record specific bioevents that occurred homotaxially within other Tethyan (e.g. Austria, Turkey, Slovakia, Sicily, Lombardian Basin) as well as extra-Tethyan stratigraphical successions (e.g. British Columbia, Nevada) (Fig. 8). In particular, the FAD of the Tethyan conodont *Misikella posthernsteini* was voted by the Task Force for the NRB in 2010 and conventionally adopted to establish the NRB (Krystyn 2010).

The appearance of the Tethyan *Misikella posthernsteini* s.s. has been correlated with the appearance of the North American *Mockina mosheri* morphotype A (e.g. Giordano *et al.* 2010; Tackett *et al.* 2014), through the appearance of both the conodont species just above the base of the radiolarian *Proparvicingula moniliformis* Zone, in particular within Assemblage 1 *sensu* Carter (1993) as stated by Carter & Orchard (2007) and Giordano *et al.* (2010) and Tackett *et al.* (2014) (Fig. 8). Moreover, the base of the *Mockina mosheri* Zone seems to coincide with the base of the North American ammonoid *Paracochloceras amoenum* Zone (e.g. Orchard & Tozer 1997). In the upper part of the radiolarian *Betraccium deweveri* Zone, the bivalve *Monotis* fauna disappeared globally: this event has been largely used to define the base of the Rhaetian, especially in the North America (Fig. 8). Instead, the rare dwarf *Monotis* specimens and thin-shelled pectinids that replaced the standard-size *Monotis* are considered Rhaetian (Wignall *et al.* 2007; McRoberts *et al.* 2008; McRoberts 2010). In fact, the dwarf *Monotis* species were found in association with ammonoids belonging to the *Paracochloceras* genus and with the conodont *M. posthernsteini* (McRoberts *et al.* 2008). The extinction of the standard-size *Monotis* species occurs at the lower boundary of the *Sagenites reticulatus* Zone (Dagys & Dagys 1994). In the Tethyan realm, the base of the *Sagenites reticulatus* Zone is considered coeval to the base of the *Paracochloceras suessi* Zone (Dagys & Dagys 1994; Krystyn *et al.* 2007a) and ex-*Cochloceras suessi* Zone *sensu* Kozur (2003) (Fig. 8). Moreover, the base of the *P. suessi* Zone seems to coincide to the FAD of the conodont *M. posthernsteini* (Kozur 2003; Krystyn & Kuerschner 2005; Krystyn *et al.* 2007a, 2007b; Moix *et al.* 2007).

In the North America, the base of the *Sagenites reticulatus* Zone correlates to the base of the ammonoid *Paracochloceras amoenum* Zone (Krystyn 1990; Dagys & Dagys 1994). Carter (1993) correlates the base of the radiolarian *Proparvicingula moniliformis* Zone with the base of the *Paracochloceras amoenum* Zone, later confirmed by Orchard *et al.* (2007) and the base of the radiolarian *Globolaxtorum tozeri* Zone with the base of the ammonoid *Choristoceras crickmayi* Zone (Carter 1993). Notably, in North America *Misikella posthernsteini* occurred in the *Choristoceras crickmayi* Ammonoid Zone (Orchard 1991; Orchard *et al.* 2007), differing from the Tethyan *Misikella posthernsteini* that instead occurs at the base of radiolarian *Proparvicingula moniliformis* Zone (Giordano *et al.* 2010), as also observed in the candidate Pignola-Abriola section (Fig. 2). The *Choristoceras crickmayi* Ammonoid Zone is considered coeval to the base of the Tethyan ammonoid *Vandaites stuerzenbaumi* Zone (Dagys & Dagys 1994; Whiteside & Ward 2011) (Fig. 8). In particular, the *Vandaites stuerzenbaumi* Zone is represented by two subzones that are the *Vandaites saximontanus* Subzone (ex-'*Choristoceras*' *haueri* Subzone) and the homonymous *Vandaites stuerzenbaumi* Subzone (Maslo 2008). Moreover, the base of the radiolarian *Globolaxtorum tozeri* seems to coincide with the base of the conodont *Misikella ultima* (Pálffy *et al.* 2007) (Fig. 8).

Around the NRB, some bioevents described above occurred in a very short time interval and therefore could be interpreted as coeval: (1) occurrence of the conodonts *Misikella posthernsteini* s.s. and *Mockina mosheri* morphotype A; (2) the occurrence of ammonoid *Paracochloceras amoenum*, which corresponds to the base of the *Sagenites reticulatus* Zone (coeval to the base of the *Paracochloceras suessi*); and (3) the base of the radiolarian *Proparvicingula moniliformis*, and the disappearance of standard-size bivalve *Monotis* spp. (Fig. 8).

These bioevents support, and are supported by, the geochemical evidence ($\delta^{13}\text{C}_{\text{org}}$) documented at Pignola-Abriola and Mt. Volturino sections around the NRB (Fig. 7).

The $\delta^{13}\text{C}_{\text{org}}$ negative shift: new proposal as primary proxy for the NRB

Even if *Misikella posthernsteini* has been voted as primary marker for the base of the Rhaetian stage (Krystyn 2010), and it is commonly used to recognize the NRB in the Tethys (Balini *et al.* 2010), *Misikella posthernsteini* appears to be rare in the North American realm, where it seems to occur in a younger stratigraphic interval than in the Tethys

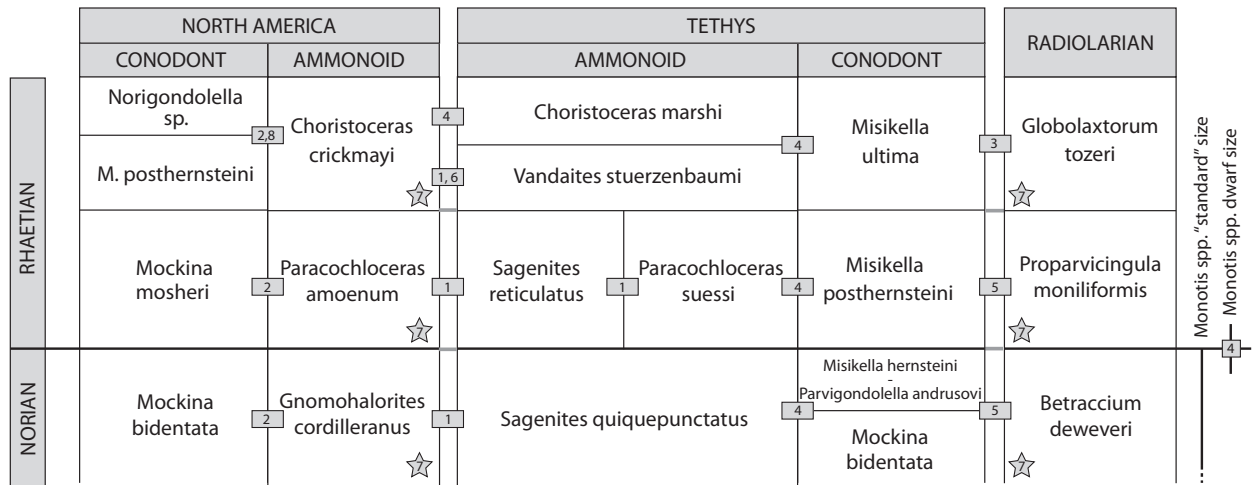


Fig. 8. Biostratigraphical correlation scheme around the NRB. References are 1. Dagys & Dagys (1994); 2. Orchard (1991); 3. Pálffy *et al.* (2007); 4. McRoberts *et al.* (2008); 5. Giordano *et al.* (2010); 6. Whiteside & Ward (2011); 7. Carter (1993); 8. Orchard *et al.* (2007).

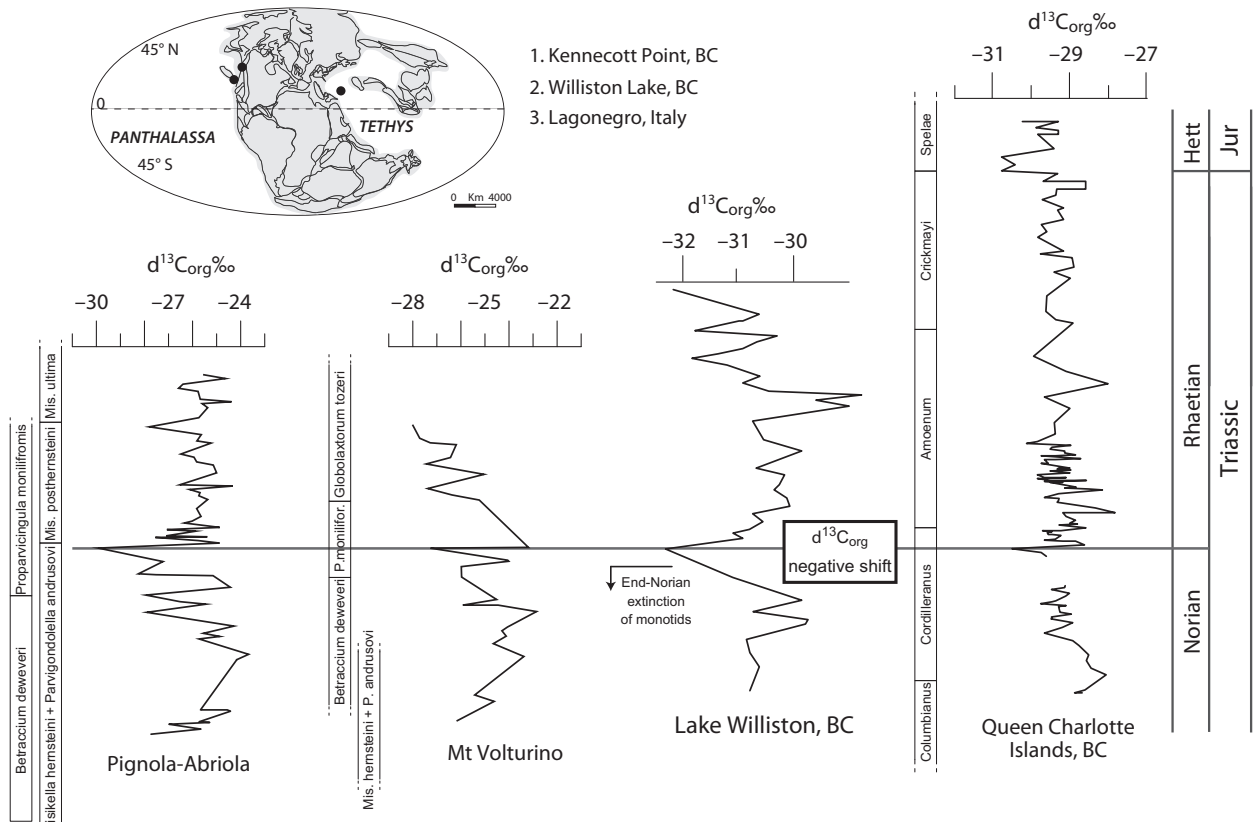


Fig. 9. Correlations of the prominent $\delta^{13}C_{org}$ negative shift considered as possible marker for the base of the Rhaetian Stage from different localities around the world: Pignola-Abriola and Mt. Volturino sections (this work, Lagonegro Basin, Italy), Lake Williston and Kenecott Point (British Columbia, Canada) (Ward *et al.* 2001, 2004; Wignall *et al.* 2007; Whiteside & Ward 2011). Paleomap is modified after scotese.com.

(Fig. 8), weakening its potential as primary tool for global correlations. For these reasons, we propose the prominent negative $\delta^{13}C_{org}$ peak occurring in

proximity of the FAD of Tethyan *Misikella posthernsteini* s.s. as the primary event to define the base of the Rhaetian stage. Notably, the organic carbon

isotope system appears unaffected by diagenetic alteration, because temperatures approaching those of oil generation are required to alter significantly the $\delta^{13}\text{C}_{\text{org}}$ primary signal (Hayes *et al.* 1999; Cramer & Saltzman 2007).

The $\delta^{13}\text{C}_{\text{org}}$ negative shift documented in the candidate Pignola-Abriola section and in the coeval Mt. Volturino section seems to correspond to similar shifts in other sections from the North American realm, such as Williston Lake (Wignall *et al.* 2007), Kennecott Point (Ward *et al.* 2001, 2004) and Frederick Island (Whiteside & Ward 2011), that are well-calibrated biostratigraphically (Fig 9). The occurrence of this negative peak also on the eastern side of the Panthalassa shows that the $\delta^{13}\text{C}_{\text{org}}$ negative shift recorded at the NRB provides a globally correlatable chronostratigraphical event and thus a useful geochemical/physical proxy in identifying the base of the Rhaetian stage (Fig. 9).

$^{87}\text{Sr}/^{86}\text{Sr}$ and $^{187}\text{Os}/^{188}\text{Os}$ datasets

A recent late Norian to Rhaetian marine $^{87}\text{Sr}/^{86}\text{Sr}$ curve based on analyses of biogenic apatite and carbonate (e.g. Korte *et al.* 2003; Cohen & Coe 2007; Callegaro *et al.* 2012; Tackett *et al.* 2014) highlights two significant shifts, one in the late Norian and one in the late Rhaetian (Fig. 10). Although Callegaro *et al.* (2012) used only conodonts with CAI < 2 for their evaluation of the Sr isotopic signal, here we include also results from conodonts with CAI = 2.5 because the threshold CAI value for the maintenance of the pristine Sr isotopic composition is precisely 2.5 (Ebneth *et al.* 1997; Korte *et al.* 2003). This curve is well mimicked by the Rhaetian seawater $^{187}\text{Os}/^{188}\text{Os}$ curve illustrated by Cohen & Coe (2002) and Kuroda *et al.* (2010) (Fig. 10). A first decreasing trend is documented in both the $^{87}\text{Sr}/^{86}\text{Sr}$ and $^{187}\text{Os}/^{188}\text{Os}$ curves, starting in the latest Norian, more precisely in the uppermost conodont *Misikella hensteini-Parvigondolella andrusovi* Zone (Callegaro *et al.* 2012) or top of the *Betracium deweveri* radiolarian Zone (Kuroda *et al.* 2010), from 0.70798 to 0.70777 for $^{87}\text{Sr}/^{86}\text{Sr}$ and from 0.6 to 0.2 for $^{187}\text{Os}/^{188}\text{Os}$ (Fig. 10). These lowest values mostly coincide with the base of the conodont *Misikella ultima* Zone, which mostly corresponds to the base of the *Globolaxtorum tozeri* radiolarian Zone (Pálffy *et al.* 2007), marking the change in trend to higher values both of the $^{87}\text{Sr}/^{86}\text{Sr}$ and $^{187}\text{Os}/^{188}\text{Os}$ curves (Fig. 10). In this context, the $\delta^{13}\text{C}_{\text{org}}$ negative shift that marks the base of the Rhaetian stage according to our proposition falls within a decreasing trend of both the $^{87}\text{Sr}/^{86}\text{Sr}$ and $^{187}\text{Os}/^{188}\text{Os}$ curves.

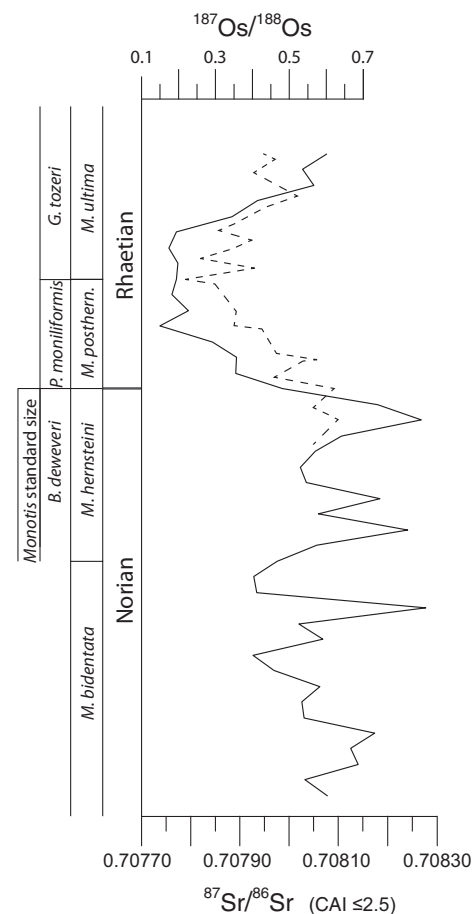


Fig. 10. Strontium and Osmium curves around the NRB (Kuroda *et al.* 2010; Callegaro *et al.* 2012) with integrated bivalve, radiolarian and conodont biostratigraphical schemes.

Conclusions

In this work, we propose the Pignola-Abriola section as candidate GSSP for the Rhaetian Stage. The Pignola-Abriola section fulfils the requirements for the selection of boundary stratotypes of chronostratigraphical units:

- 1 The Pignola-Abriola section is well exposed in an area of minimal structural deformation with easy access along the SS 5 road 'la Sellata' and is located in the protected area of the Parco Appennino Lucano Val d'Agri Lagonegrese.
- 2 The Pignola-Abriola section is a continuous 63-m-thick basinal succession, consisting of thinly bedded cherty limestones, shales and sparse layers of calcarenites (Calcarì con Selce Fm), deposited in the Lagonegro Basin (Southern Apennines).
- 3 The Pignola-Abriola section is fossiliferous, with distinctive and well-preserved conodont and radiolarian cosmopolitan fauna; the FAD of the con-

odont *Misikella posthernsteini* s.s. and the base of the radiolarian *Proparvicungula moniliformis* Zone, which are two bioevents suggested to mark the base of the Rhaetian, are well-documented and intercalibrated.

- 4 The Pignola-Abriola section shows a marked negative $\delta^{13}\text{C}_{\text{org}}$ excursion of ca. 6‰ within an overall decreasing trend, and that is mirrored by a negative shift of $\delta^{13}\text{C}_{\text{carb}}$ curve, occurring ca. 0.5 metres below the FAD of *M. posthernsteini* s.s. and within the radiolarian *P. moniliformis* Zone. This negative carbon isotope shift is here suggested as the primary physical marker for the Norian/Rhaetian boundary.
- 5 The Pignola-Abriola section is subdivided into 10 magnetozones, calibrated with conodont and radiolarian biostratigraphy and statistically correlated with the Newark APTS.

Acknowledgements. – We are indebted to G. Ciarapica, L. Passeri, N. Giordano, N. Preto and G. Roghi for discussion and assistance in field during the last 10 years. Thanks to Ing. Donato Rosa, Ing. Mancusi, Geom. Pietrafesa (Department for Environment, Town Planning and Building of the Pignola district) and to Ignazio Petrone, Mayor of Pignola (Potenza) in the 2011. Thanks also to the Corpo Forestale dello Stato – Stazione di Pignola and to Ing. Domenico Totaro, President of the Appennino Lucano National Park. We thank the editor, the anonymous reviewer and the Chairman of the Subcommittee on Triassic Stratigraphy (ICS) Prof. Marco Balini (Milano University) for their constructive comments on the manuscript. This study has benefited from financial support of Progetto d'Ateneo 2009 (CPDA090175/09 to Rigo), and Ex 60% (60A05-2288/09 and 60A05-3279/13 to Rigo) and PRIN Preto (20107ESMX9_002), PRIN 2008 2008BEF5Z7_004 to Bertinelli and 2008BEF5Z7_005 to Rigo. Acknowledgement is made to the donors of the American Chemical Society Petroleum Research Fund for partial support of this research (grant 49637-DN18 to Katz). Stable isotope analyses were funded through NSF grant EAR 0844252 to Godfrey.

References

- Ager, D.V. 1987: A defense of the Rhaetian Stage. *Albertiana* 6, 4–13.
- Amodeo, F. 1999: Il Triassico terminale–Giurassico del Bacino Lagonegrese. Studi stratigrafici sugli Scisti Silicei della Basilicata (Italia meridionale). *Mémoires de Géologie (Lausanne)* 33, 1–123.
- Amodeo, F., Molisso, F., Kozur, H., Marsella, E. & D'Argenio, B. 1993: Age of transitional beds between Cherty Limestones (Calcarei con Selce) and Radiolarites (Scisti Silicei) in the Lagonegro domain (Southern Italy). First evidence of Rhaetian Conodonts in Peninsular Italy. *Bollettino Servizio Geologico Italiano* 110, 3–22.
- von Arthaber, G. 1905: Die alpine Trias des Mediterran Gebietes. In Frech, F. (ed.): *Trias Lethea Geognostica, Part 2, Das Mesozoicum. Schweizerbart, Stuttgart*, 1–623.
- Balini, M., Lucas, S.G., Jenks, J.F. & Spielmann, J.A. 2010: Triassic ammonoid biostratigraphy: an overview. In Lucas, S.G. (ed.): *The Triassic Timescale. Geological Society, London, Special Publications* 334, 221–262.
- Bazzucchi, P., Bertinelli, A., Ciarapica, G., Marcucci, M., Passeri, L., Rigo, M. & Roghi, G. 2005: The Late Triassic–Jurassic stratigraphic succession of Pignola (Lagonegro–Molise Basin, Southern Apennines, Italy). *Bollettino Società Geologica Italiana* 124, 143–153.
- Bertinelli, A., Ciarapica, G., De Zanche, V., Marcucci, M., Passeri, L., Rigo, M. & Roghi, G. 2005a: Stratigraphic evolution of the Triassic–Jurassic Sasso di Castalda succession (Lagonegro basin, Southern Apennines, Italy). *Bollettino Società Geologica Italiana* 124, 161–175.
- Bertinelli, A., Ciarapica, G. & Passeri, L. 2005b: Late Triassic–Jurassic basinal successions in Molise and northern Basilicata: the northernmost witness of the Lagonegro domain. *Bollettino Società Geologica Italiana* 124, 177–188.
- Callegaro, S., Rigo, M., Chiaradia, M. & Marzoli, A. 2012: Latest Triassic marine Sr isotopic variations, possible causes and implications. *Terra Nova* 24, 130–135.
- Carter, E.S. 1993: Biochronology and Paleontology of uppermost Triassic (Rhaetian) radiolarians, Queen Charlotte Islands, British Columbia, Canada. *Mémoires de Géologie (Lausanne)* 11, 1–176.
- Carter, E.S. & Orchard, M.J. 2007: Radiolarian – conodont – ammonoid intercalibration around the Norian–Rhaetian Boundary and implications for trans–Panthalassan correlation. *Albertiana* 36, 149–163.
- Catalano, R., Doglioni, C. & Merlini, S. 2001: On the Mesozoic Ionian basin. *Geophysical Journal International* 144, 49–64.
- Channell, J.E.T., Kozur, H.W., Sievers, T., Mock, R., Aubrecht, R. & Sykora, M. 2003: Carnian–Norian biomagnetostratigraphy at Šilická Brezová (Slovakia): Correlation to other Tethyan sections and to Newark Basin. *Palaeogeography, Palaeoclimatology, Palaeoecology* 191, 65–109.
- Ciarapica, G. & Passeri, L. 2002: The palaeogeographic duplicity of the Apennines. *Bollettino Della Società Geologica Italiana* 121, 67–75.
- Ciarapica, G. & Passeri, L. 2005: Ionian tethydes in the Southern Apennines. In Finetti, I.R. (ed): *Crop Project: Deep Seismic Exploration of the Central Mediterranean and Italy*, 209–224. Elsevier, Amsterdam.
- Ciarapica, G., Cirilli, S., Panzanelli Fratoni, R., Passeri, L. & Zaninetti, L. 1990: The Mt. Facito Formation (Southern Apennines). *Bollettino Società Geologica Italiana* 109, 135–142.
- Cohen, A.S. & Coe, A.L. 2002: New geochemical evidence for the onset of volcanism in the Central Atlantic magmatic province and environmental change at the Triassic–Jurassic boundary. *Geology* 30, 267–270.
- Cohen, A.S. & Coe, A.L. 2007: The impact of the Central Atlantic Magmatic Province on climate and on the Sr- and Os-isotope evolution of seawater. *Palaeogeography, Palaeoclimatology, Palaeoecology* 244, 374–390.
- Coplen, T.B., Brand, W.A., Gehre, M., Gröning, M., Meijer, H.A.J., Toman, B. & Verkouteren, R.M. 2006: New guidelines for $\delta^{13}\text{C}$ measures. *Analytical Chemistry* 78, 2439–2441.
- Cramer, B.D. & Saltzman, M.R. 2007: Early Silurian paired $\delta^{13}\text{C}_{\text{carb}}$ and $\delta^{13}\text{C}_{\text{org}}$ analyses from the Midcontinent of North America: Implications for paleoceanography and paleoclimate. *Palaeogeography, Palaeoclimatology, Palaeoecology* 256, 195–203.
- Dagys, A.S. & Dagys, A.A. 1994: Global correlation of the terminal triassic. In Guex, J., Baud, A. (eds): *Recent Developments on Triassic Stratigraphy. Mémoires de Géologie, Lausanne* 22, 25–34.
- De Capoa, P. 1970: Le Daonelle e le Halobie della serie calcareo-siliceo-marnosa della Lucania (Appennino Meridionale). Studio paleontologico e biostratigrafico. *Società Naturale Napoli, Suppl. Bollettino* 78, 1–127.
- De Capoa, P. 1984: *Halobia* zones in the pelagic Late Triassic sequences of the central Mediterranean area (Greece, Yugoslavia, Southern Apennines, Sicily). *Bollettino Società Paleontologica Italiana* 23, 91–102.
- De Lorenzo, G. 1894: Le Montagne mesozoiche di Lagonegro. *Reale Accademia Delle Scienze Fisiche e Matematiche di Napoli* 00, 1–124.
- De Wever, P. & Miconnet, P. 1985: Datations directes des radiolarites du bassin de Lagonegro (Lucanie, Italie méridionale).

- Implications et conséquences. *Rivista Espanola De Micropaleontologia* 17, 373–402.
- Ebneth, S., Diener, A., Buhl, D. & Veizer, J. 1997: Strontium isotope systematics of conodonts: middle Devonian, Eifel Mountains, Germany. *Palaeogeography, Palaeoclimatology, Palaeoecology* 132, 79–96.
- Epstein, A.G., Epstein, J.B. & Harris, L.D. 1977: Conodont color alteration an index to organic metamorphism. *US Geological Survey Professional Paper* 995, 1–27.
- Fähræus, L.E. & Ryley, C. 1989: Multielement species of *Misikella* Kozur and Mock, 1974 and *Axiothea* n. gen. (Conodonta) from the Mamonia Complex (Upper Triassic), Cyprus. *Canadian Journal of Earth Sciences* 26, 1255–1263.
- Gallet, Y., Krystyn, L., Marcoux, J. & Besse, J. 2007: New constraints on the End-Triassic (Upper Norian-Rhaetian) magnetostratigraphy. *Earth and Planetary Science Letters* 255, 458–470.
- Gardin, S., Krystyn, L., Richoz, S., Bartolini, A. & Galbrun, B. 2012: Where and when the earliest coccolithophores? *Lethaia* 45, 507–523.
- Gaździcki, A. 1978: Conodonts of the genus *Misikella* Kozur & Mock, 1974 from the Rhaetian of the Tatra Mts (West Carpathians). *Acta Palaeontologica Polonica* 23, 341–354.
- Gaździcki, A., Kozur, H. & Mock, R. 1979: The Norian-Rhaetian boundary in the light of micropaleontological data. *Geologija* 22, 71–112.
- Giordano, N., Rigo, M., Ciarapica, G. & Bertinelli, A. 2010: New biostratigraphical constraints for the Norian/Rhaetian boundary: data from Lagonegro Basin, Southern Apennines, Italy. *Lethaia* 43, 573–586.
- Giordano, N., Ciarapica, G., Bertinelli, A. & Rigo, M. 2011: The Norian-Rhaetian interval in two sections of the Lagonegro area: the transition from carbonate to siliceous deposition. *Italian Journal of Geoscience* 130, 380–393.
- Gradstein, F.M., Ogg, J.G., Schmitz, M. & Ogg, G. 2012: *The Geological Time Scale 2012*, 1–1142. Elsevier, Amsterdam.
- Grant-Mackie, J.A. 1978: Subgenera of the Upper Triassic Bivalve *Monotis*. *New Zealand Journal of Geology and Geophysics* 21, 97–111.
- Guembel, C.W. 1861: *Geognostische Beschreibung des Bayerischen Alpengebirges und Seine Vorlandes*, 1-950. Perthes, Gotha.
- Guex, J., Schoene, B., Bartolini, A., Spangenberg, J., Schaltegger, U., O'Dogherty, L., Taylor, D., Bucher, H. & Atudorei, V. 2012: Geochronological constraints on post-extinction recovery of the ammonoids and carbon cycle perturbation during the Early Jurassic. *Palaeogeography, Palaeoclimatology, Palaeoecology* 346–347, 1–11.
- Hayes, J.M., Strauss, H. & Kaufman, A.J. 1999: The abundance of ^{13}C in marine organic matter and isotopic fractionation in the global biogeochemical cycle of carbon during the past 800 Ma. *Chemical Geology* 161, 103–125.
- Hesselbo, S.P., Robinson, S.A., Surlyk, F. & Piasecki, S. 2002: Terrestrial and marine extinction at the Triassic-Jurassic boundary synchronized with major carbon-cycle perturbation: a link to initiation of massive volcanism? *Geology* 30, 251–254.
- Higgins, J.A. & Schrag, D.P. 2006: Beyond methane: towards a theory for the Paleocene–Eocene thermal maximum. *Earth Planetary Science Letters* 245, 523–537.
- Hounslow, M.W. & Muttoni, G. 2010: The geomagnetic polarity timescale for the Triassic: linkage to stage boundary definitions. In Lucas, S.G. (ed.): *The Triassic Timescale*. Geological Society, London, Special Publications 334, 61–102.
- Hüsing, S.K., Deenen, M.H.L., Koopmans, J.G. & Krijgsman, W. 2011: Magnetostratigraphic dating of the proposed Rhaetian GSSP at Steinbergkogel (Upper Triassic, Austria): implications for the Late Triassic time scale. *Earth and Planetary Science Letters* 302, 203–216.
- Jenkyns, H.C. 2010: Geochemistry of oceanic anoxic events. *Geochemistry Geophysics Geosystems* 11, 1–30.
- Korte, C., Kozur, H.W., Bruckschen, P. & Veizer, J. 2003: Strontium isotope evolution of Late Permian and Triassic seawater. *Geochimica, Cosmochimica Acta* 67, 47–62.
- Kozur, H.W. 2003: Integrated Permian ammonoid, conodont and radiolarian zonation of the Triassic. *Hallesches Jahrbuch für Geowissenschaften* 25, 49–79.
- Kozur, H. & Mock, R. 1974: *Misikella posthernsteini* n. sp., die jüngste Conodontenart der tethyalen Trias. *Càsopsis pro Mineralogii a Geologii* 19, 245–250.
- Kozur, H. & Mock, R. 1991: New Middle Carnian and Rhaetian conodonts from Hungary and the Alps, stratigraphic importance and tectonic implications for the Buda Mountains and adjacent areas. *Jahrbuch der Geologischen Bundesanstalt* 134, 271–297.
- Krystyn, L. 1980: Stratigraphy of the Hallstatt region. *Guidebook, Abstracts, Second European Conodont Symposium- ECOS II, Abhandlungen Geologie B.-A.* 35, 69–98.
- Krystyn, L. 1990: A Rhaetian stage-chronostratigraphy, subdivision and their intercontinental correlation. *Albertiana* 8, 15–24.
- Krystyn, L. 2008: The Hallstatt pelagics – Norian and Rhaetian Fossilagerstaetten of Hallstatt. *Berichte der Geologische Bundesanstalt-A.* 76, 81–98.
- Krystyn, L. 2010: Decision report on the defining event for the base of the Rhaetian stage. *Albertiana* 38, 11–12.
- Krystyn, L. & Kuerschner, W. 2005: Biotic events around the Norian-Rhaetian boundary from a Tethyan perspective. *Albertiana* 32, 17–20.
- Krystyn, L., Bouquerel, H., Kuerschner, W., Richoz, S. & Gallet, Y. 2007a: Proposal for a candidate GSSP for the base of the Rhaetian stage. In Lucas, S.G., Spielman, J.A. (eds): *The Global Triassic*. New Mexico Museum of Natural History and Science Bulletin 41, 189–199.
- Krystyn, L., Richoz, S., Gallet, Y., Bouquerel, H., Kuerschner, W.M. & Spötl, C. 2007b: Updated bio- and magnetostratigraphy from Steinbergkogel (Austria), candidate GSSP for the base of the Rhaetian stage. *Albertiana* 36, 164–173.
- Kuroda, J., Hori, R.S., Suzuki, K., Grocke, D.R. & Ohkouchi, N. 2010: Marine osmium isotope record across the Triassic-Jurassic boundary from a Pacific pelagic site. *Geology* 38, 1095–1098.
- Maron, M., Rigo, M., Bertinelli, A., Katz, M.E., Godfrey, L., Zafani, M. & Muttoni, G. 2015: Magnetostratigraphy, biostratigraphy and chemostratigraphy of the Pignola-Abriola section: new constraints for the Norian/Rhaetian boundary. *Geological Society of America Bulletin* doi: 10.1130/B31106.1.
- Maslo, M. 2008: Taxonomy and Stratigraphy of the Upper Triassic heteromorphic ammonoids: preliminary results from Austria. *Berichte der Geologische Bundesanstalt-A.* 76, 15–16.
- Mazza, M., Rigo, M. & Gullo, M. 2012: Taxonomy and biostratigraphic record of the Upper Triassic conodonts of the Pizzo Mondello section (Western Sicily, Italy), GSSP candidate for the base of the Norian. *Rivista Italiana di Paleontologia e Stratigrafia* 118, 85–130.
- McFadden, P.L. & McElhinny, M.W. 1990: Classification of the reversal test in palaeomagnetism. *Geophysical Journal International* 103, 725–729.
- McRoberts, C.A. 2010: Biochronology of Triassic bivalves. *Geological Society of London, Special Publications* 334, 201–219.
- McRoberts, C.A., Krystyn, L. & Shea, A. 2008: Rhaetian (Late Triassic) *Monotis* (Bivalvia: Pectinoida) from the eastern Northern Calcareous Alps (Austria) and the end-Norian crisis in pelagic faunas. *Palaeontology* 51, 721–735.
- Meyer, P.A. 2014: Why are the $\delta^{13}\text{C}_{\text{org}}$ values in the Phanerozoic black shales more negative than in modern marine organic matter? *Geochemistry, Geophysics, Geosystems* 15, 3085–3106.
- Miconnet, P. 1982: Précisions stratigraphiques et tectoniques dans un secteur du Lagonegro (Italie méridionale). *Annales de la Société Géologique du Nord* 102, 17–24.
- Moix, P., Kozur, H.W., Stampfli, G.M. & Mostler, H. 2007: New paleontological, biostratigraphic and paleogeographic results from the Triassic of the Mersin Mélange, SE Turkey. In Lucas, S.G., Spielmann, J.A. (eds): *The Global Triassic*. New Mexico Museum of Natural History and Science Bulletin 41, 282–311.

- Mostardini, F. & Merlini, S. 1986: Appennino centro-meridionale. Sezioni geologiche e proposta di modello strutturale. *Memorie Società Geologica Italiana* 35, 177–202.
- Mostler, H., Scheuring, B. & Urlichs, M. 1978: Zur Mega-, Mikrofauna und Mikroflora der Kössener Schichten (alpine Obertrias) vom Weissloferbach in Tirol unter besonderer Berücksichtigung der in der *suessi-* und *marshi-* Zone auftretenden Conodonten. *Schrift. Erdwiss. Schriftenreihe der Erdwissenschaftlichen Kommissionen* 4, 141–174.
- Muttoni, G., Kent, D.V., Olsen, P.E., Di Stefano, P., Lowrie, W., Bernasconi, S.M. & Hernandez, F.M. 2004: Tethyan magnetostratigraphy from Pizzo Mondello (Sicily) and correlation to the Late Triassic Newark astrochronological polarity time scale. *Geological Society of America Bulletin* 116, 1043–1058.
- Muttoni, G., Kent, D.V., Jadoul, F., Olsen, P.E., Rigo, M., Galli, M.T. & Nicora, A. 2010: Rhaetian magneto-biostratigraphy from the Southern Alps (Italy): constraints on Triassic chronology. *Palaeogeography, Palaeoclimatology, Palaeoecology* 285, 1–16.
- Muttoni, G., Mazza, M., Mosher, D., Katz, M.E., Kent, D.V. & Balini, M. 2014: A Middle-Late Triassic (Ladinian-Rhaetian) carbon and oxygen isotope record from the Tethyan Ocean. *Palaeogeography, Palaeoclimatology, Palaeoecology* 399, 246–259.
- O'Dogherty, L., Carter, E.S., Dumitrica, P., Goričan, Š. & De Wever, P. 2009: An illustrated and revised catalogue of Mesozoic radiolarian genera – objectives, concepts and guide for users. *Geodiversitas* 31, 191–212.
- Olsen, P.E., Kent, D.V. & Whiteside, J.H. 2011: Implications of the Newark Supergroup-based astrochronology and geomagnetic polarity time scale (Newark-APTS) for the tempo and mode of the early diversification of the Dinosauria. *Earth and Environmental Science Transactions of the Royal Society of Edinburgh* 101, 201–229.
- Orchard, M.J. 1991: Upper Triassic conodont biochronology and new index species from the Canadian Cordillera. *Geological Survey of Canada, Bulletin* 417, 299–335.
- Orchard, M.J. & Tozer, E.T. 1997: Triassic conodont biochronology, its calibration with the ammonoid standard, and a biostratigraphic summary for the Western Canada Sedimentary Basin. *Bulletin of Canadian Petroleum Geology* 45, 675–692.
- Orchard, M.J., Carter, E.S., Lucas, S.G. & Taylor, D.G. 2007: Rhaetian (Upper Triassic) conodonts and radiolarians from New York Canyon, Nevada, USA. *Albertiana* 35, 59–65.
- Pálffy, J., Demeny, A., Haas, J., Carter, E.S., Gorog, A., Halasz, D., Oravecz-Scheffer, A., Hetenyi, M., Marton, E., Orchard, M.J., Ozsvart, P., Veto, I. & Zsai, N. 2007: Triassic-Jurassic boundary events inferred from integrated stratigraphy of the Csovar section, Hungary. *Palaeogeography, Palaeoclimatology, Palaeoecology* 224, 11–33.
- Palmer, A.R. 1983: The Decade of North American Geology 1983 geological time scale. *Geology* 11, 503–504.
- Passeri, L., Bertinelli, A. & Ciarapica, G. 2005: Palaeogeographic meaning of the late Triassic-Early Jurassic Lagonegro units. *Bollettino Società Geologica Italiana* 124, 231–245.
- Pearson, D.A.B. 1970: Problems of Rhaetian stratigraphy with special reference to the lower boundary of the stage. *Journal of the Geological Society London* 146, 125–150.
- Preto, N., Agnini, C., Rigo, M., Sprovieri, M. & Westphal, H. 2013: The calcareous nannofossil *Prinsiosphaera* achieved rock-forming abundances in the latest Triassic of western Tethys: consequences for the ^{13}C of bulk carbonate. *Biogeosciences* 10, 6053–6068.
- Reggiani, L., Bertinelli, A., Ciarapica, G., Marcucci, M., Passeri, L., Ricci, C. & Rigo, M. 2005: Triassic-Jurassic stratigraphy of the Madonna del Sirino succession (Lagonegro basin, Southern Apennines, Italy). *Bollettino Società Geologica Italiana* 124, 281–291.
- Remane, J. 2003: Chronostratigraphic correlations: their importance for the definition of geochronologic units. *Palaeogeography, Palaeoclimatology, Palaeoecology* 196, 7–18.
- Rigo, M. & Joachimski, M.M. 2010: Palaeoecology of Late Triassic conodonts: constraints from oxygen isotopes in biogenic apatite. *Acta Palaeontologica Polonica* 55, 471–478.
- Rigo, M., De Zanche, V., Mietto, P., Preto, N. & Roghi, G. 2005: Biostratigraphy of the Calcari con Selce formation. *Bollettino Società Geologica Italiana* 124, 293–300.
- Rigo, M., Preto, N., Roghi, G., Tateo, F. & Mietto, P. 2007: A rise in the Carbonate Compensation Depth of western Tethys in the Carnian (Late Triassic): deep-water evidence for the Carnian Pluvial Event. *Palaeogeography, Palaeoclimatology, Palaeoecology* 246, 188–205.
- Rigo, M., Trotter, J., Preto, N. & Williams, I. 2012a: Oxygen isotopic evidence for Late Triassic monsoonal upwelling in the northwestern Tethys. *Geology* 40, 515–518.
- Rigo, M., Preto, N., Franceschi, M. & Guaiumi, C. 2012b: Stratigraphy of the Carnian-Norian Calcari con Selce Formation in the Lagonegro Basin, Southern Apennines. *Rivista Italiana di Paleontologia e Stratigrafia* 118, 143–154.
- Scandone, P. 1967: Studi di geologia lucana: la serie calcareo-silicomarnosa. *Bollettino Società Naturalisti Napoli* 76, 1–175.
- Schlanger, S.O. & Jenkyns, H.C. 1976: Cretaceous oceanic anoxic events: causes and consequences. *Geologie en Mijnbouw* 55, 179–184.
- Schoene, B., Guex, J., Bartolini, A., Schaltegger, U. & Blackburn, T.J. 2010: A correlation between the Triassic-Jurassic boundary mass extinction and flood basalt eruption at the 100-ka level using ID-TIMS U/Pb zircon geochronology. *Geology* 38, 387–390.
- Şengör, A.M.C., Yilmaz, Y. & Sungurlu, O. 1984: Tectonics of the Mediterranean Cimmerides: nature and evolution of the western termination of Palaeo-Tethys. *Geological Society, London, Special Publications* 17, 77–112.
- Silberling, N.J. & Tozer, E.T. 1968: Biostratigraphic classification of the marine Triassic in North America. *Geological Society of America Special Paper* 110, 1–63.
- Slavin, V.I. 1961: Stratigraphic position of the Rhaetian Stage. *Sovetskaya Geologiya* 3, 68–78.
- Slavin, V.I. 1963: Au sujet du Rhétien. *Bureau Recherches Géologie et Minières Memoir* 15, 29–32.
- Stampfli, G.M. & Marchant, R.H. 1995: Plate configuration and kinematics in the Alpine region. *Accademia Nazionale Delle Scienze, Scritti e Documenti* 14, 147–166.
- Stampfli, G., Marcoux, J. & Baud, A. 1991: Tethyan margins in space and time. *Palaeogeography, Palaeoclimatology, Palaeoecology* 87, 373–409.
- Tackett, L.S., Kaufman, A.J., Corsetti, F.A. & Bottjer, D.J. 2014: Strontium isotope stratigraphy of the Gabbs Formation (Nevada): implications for global Norian-Rhaetian correlations and faunal turnover. *Lethaia* 47, 500–511.
- Tanner, L.H. 2010: The Triassic isotope record. In Lucas, S.G. (ed.): *The Triassic Timescale*. Geological Society, London, *Special Publications* 334, 103–118.
- Tozer, E.T. 1967: A standard for Triassic time. *Geological Survey of Canada Bulletin* 156, 1–45.
- Tozer, E.T. 1979: Latest Triassic ammonoid faunas and biochronology, Western Canada. *Current Research, Part B, Geological Survey of Canada, Paper* 79-1B, 127–135.
- Tozer, E.T. 1984: The Trias and its ammonoids: the evolution of a time scale. *Geological Survey of Canada Miscellaneous Report* 35, 1–171.
- Tozer, E.T. 1990: How many Rhaetians? *Albertiana* 8, 10–13.
- Trotter, A.J., Williams, S.I., Nicora, A., Mazza, M. & Rigo, M. 2015: Long-term cycles of Triassic climate change: a new $\delta^{18}\text{O}$ record from conodont apatite. *Earth and Planetary Science Letters* 415, 165–174.
- Von Mojsisovics, E., Waagen, W.H. & Diener, C. 1895: Entwurf einer Gliederung der pelagischen Sediments des Trias-Systems. *Akademie Wissenschaft Wien, Mathematische-Naturwissenschaftliche Klasse Sitzungsberichte* 104, 1279–1302.
- Ward, P.D., Haggart, J.W., Carter, E.S., Wilbur, D., Tipper, H.W. & Evans, T. 2001: Sudden productivity collapse associated with the Triassic-Jurassic boundary mass extinction. *Science* 292, 1148–1151.

- Ward, P.D., Garrison, G.H., Haggart, J.W., Kring, D.A. & Beattie, M.J. 2004: Isotopic evidence bearing on Late Triassic extinction events, Queen Charlotte Islands, British Columbia, and implications for the duration and cause of the Triassic-Jurassic mass extinction. *Earth Planetary Science Letters* 224, 589–600.
- Whiteside, J. & Ward, P.D. 2011: Ammonoid diversity and disparity track episodes of chaotic carbon cycling during the early Mesozoic. *Geology* 39, 99–102.
- Wignall, P.B., Zonneveld, J.-P., Newton, R.J., Amor, K., Sephton, M.A. & Hartley, S. 2007: The end Triassic mass extinction record of Williston Lake, British Columbia. *Palaeogeogr. Palaeoclimatol. Paleoecol.* 253, 385–406.
- Wotzlaw, J.F., Guex, J., Bartolini, A., Gallet, Y., Krystyn, L., McRoberts, C.A., Taylor, D., Schoene, B. & Schaltegger, U. 2014: Towards accurate numerical calibration of the Late Triassic: high precision U-Pb geochronology constraints on the duration of the Rhaetian. *Geology* 42, 571–574.
- Zapfe, H. 1974: Die stratigraphie der alpin-mediterranean trias. *Schriftenreihe Erdwissenschaftlichen Kommissionen Osterreichische Akademie der Wissenschaften* 2, 1–324.
- Zapfe, H. 1983: Das Forschungsprojekt “Triassic of the Tethys Realm” (IGCP Project 4) (Abschlussbericht). *Schriftenreich Erdwissenschaftlichen Komitee* 5. Wien: Oesterreiche Akademie der Wissenschaft.